Chapter 2
Signal Amplification for Nanobiosensing

2.1 Introduction

One of the major goals in developing novel biological assay methods for the detection of biomolecules and DNA hybridization is achieving high sensitivity. The need for ultrasensitive bioassays is of major importance in view of the growing trend toward miniaturized assays. Highly sensitive methods, which are urgently required for measuring disease diagnosis markers present at ultralow levels during early stages of disease progression, can facilitate the treatment of diseases. For example, polymerase chain reaction (PCR) amplification has revolutionized genetic testing. However, it is somewhat restricted because of its complexity, potential contamination, and cost. On the other hand, the ultrasensitive monitoring of proteins is particularly challenging due to the absence of PCR-like amplification protocols. Conventional (optical and electronic) sandwich bioaffinity assays have the disadvantage of capturing a small number of labels per binding event. Recently, signal amplification has attracted considerable attention for developing ultrasensitive detection methods for biothreats and infectious agents. Such kinds of highly sensitive bioagent detection schemes provide an early warning of their release and prevent outbreaks of foodborne illnesses, hence minimizing human casualties.

The achievement of ultrahigh sensitivity requires innovative approaches that couple with different amplification platforms and amplification processes. Nanotechnology offers unique opportunities for creating highly sensitive innovative biosensing devices and ultrasensitive bioassays. The unique optical [1–4], photophysical [5], electronic [6], and catalytic [7–9] properties of metal and semiconductor nanoparticles (NPs) turn them into ideal labels for biorecognition and biosensing processes. For example, the unique plasmon-absorbance features of gold (Au) NPs and specifically the interparticle-coupled plasmon absorbance of conjugated particles have been widely used for DNA [10] and antibody–antigen [11–13] analyses. Similarly, the tunable fluorescence properties of semiconductor NPs have

H. Ju et al., *NanoBiosensing: Principles, Development and Application*,
Biological and Medical Physics, Biomedical Engineering,
DOI 10.1007/978-1-4419-9622-0_2, © Springer Science+Business Media, LLC 2011

been used for the photonic detection of biorecognition processes [14]. This chapter focuses on signal amplification based on nanobiotechnologies for highly sensitive nanobiosensing.

2.2 Nanoparticle-Amplified Optical Assay

Among all detection methods used in biosensors, the optical-based technique is the most popular one because of its high sensitivity and the ability to remotely interrogate the information on the biosensor using light or laser. Metal NPs, such as Au and silver NPs, exhibit plasmon absorbance bands in the visible spectral region that are controlled by the size of the respective particles. Numerous studies on the labeling of biomaterials and the staining of biological tissues by metal particles as a means to image and visualize biological processes have been reported [15, 16]. The spectral shifts originating from adjacent or aggregated metal NPs, such as Au NPs [17], have led to increasing interest in the development of optical biosensors based on biomaterial-NP hybrid systems. Similarly, semiconductor NPs exhibit size-dependent tunable absorbance and fluorescence. Due to the high-fluorescence quantum yields, photostability, and tunable fluorescence bands, semiconductor NPs are attracting substantial research interest as fluorescence labels for biorecognition processes.

2.2.1 Colloidal Gold Nanoparticle-Based Amplification

The unique plasmon-absorbance features of Au NPs, and specifically the interparticle-coupled plasmon absorbance of conjugated particles, have been widely used for DNA [18] and antibody–antigen [19–22] analyses. For example, a cationic Au NP has been used for signal amplification by ionic interaction with 16S rRNA hybridized on the peptide nucleic acid probe-immobilized surface plasmon resonance (SPR) sensor chip [23]. Peptide nucleic acid has a neutral backbone structure; therefore, hybridization with 16S rRNA results in the ionic condition being changed from neutral to negative. 16S rRNA has been used as a genetic marker for the identification of organisms and can be analyzed directly without PCR amplification due to the relatively high number of copies. This method results in an *Escherichia coli* rRNA detection limit of 58.2 (±1.37) pg/mL. With this analytical method, *Staphylococcus aureus* can be detected without purification of rRNA. Yao et al. [24] used oligonucleotide (ODN)-capped Au NPs in a sandwich assay of ODN or polynucleotide by flow-injection SPR. A carboxylated dextran film was immobilized onto the SPR sensor surface to eliminate the nonspecific adsorption of ODN-capped Au NPs. The tandem use of signal amplification via the adlayer of the ODN-capped Au NPs and the differential signal detection by the bicell detector on the SPR resulted in a remarkable detection limit of DNA. A 39-mer target at a quantity as low as 2.1×10^{-20} mol, corresponding to 1.38 fM, can be measured. The method is shown to be reproducible (relative standard deviation values <16%) and to possess high sequence specificity. Drastic sensitivity enhancement

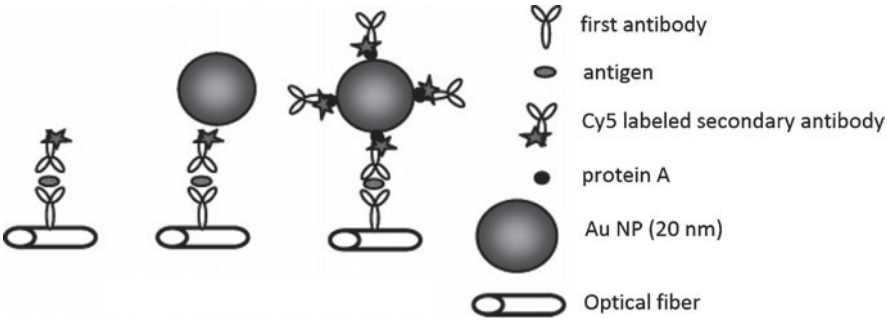

Fig. 2.1 Diagram of the three types of fluorescence probes used for the LSPCF biosensor. Reprinted with permission from Hsieh et al. [27]. © 2007, American Chemical Society

was maximized using longitudinal plasmonic resonance of Au nanorods for ultrasensitive SPR biosensing with functionalized Au nanorods as amplification labels due to the electromagnetic interaction between the nanotag and the sensing film [25, 26]. The detection sensitivity of the nanorod-conjugated antibody was estimated to be ~40 pg/mL, which was 25–100 times more sensitive than the current reported values. A novel fiber optic biosensor based on a localized surface plasmon-coupled fluorescence (LSPCF) system also has been developed [27]. As shown in Fig. 2.1, the biosensor consists of a biomolecular complex in a sandwich format of antibody/antigen/Cy5–antibody–Au NP. It is immobilized on the surface of an optical fiber, where a Cy5–antibody–Au NP complex forms the fluorescence probe. The LSPCF is excited by localized surface plasmon on the Au NP's surface, where the evanescent field is applied near the core surface of the optical fiber. At the same time, the fluorescence signal is detected, with high collection efficiency, by a photomultiplier tube located beside the unclad optical fiber. This LSPCF biosensor is able to detect mouse immunoglobulin G (IgG) as low as 1 pg/mL (7 fM) during the biomolecular interaction of the IgG with antimouse IgG, indicating a very high sensitivity due to the amplification of the LSPCF intensity by Au NP coupling.

A highly sensitive and specific colorimetry-based rolling-circle amplification (RCA) assay method for single-nucleotide polymorphism (SNP) genotyping has been developed [28]. As shown in Fig. 2.2, a circular template is generated by ligation upon the recognition of a point mutation on DNA targets. An RCA amplification is then initiated using the circular template in the presence of Phi29 polymerase. The RCA product can be digested by a restricting endonuclease, and the cleaved DNA fragments can mediate the aggregation of Au NP-tagged DNA probes. This causes a colorimetric change of the solution as the indicator of the mutation occurrence, which can be detected using UV-vis spectroscopy or viewed by naked eyes. On the basis of the high amplification efficiency of Phi29 polymerase, a mutated target of 70 fM can be detected in this assay. In addition, the protection of the circle template using phosphorothioated nucleotides allows the digestion reaction to be performed simultaneously in RCA. Moreover, DNA ligase offers high fidelity in distinguishing the mismatched bases at the ligation site, resulting in the positive

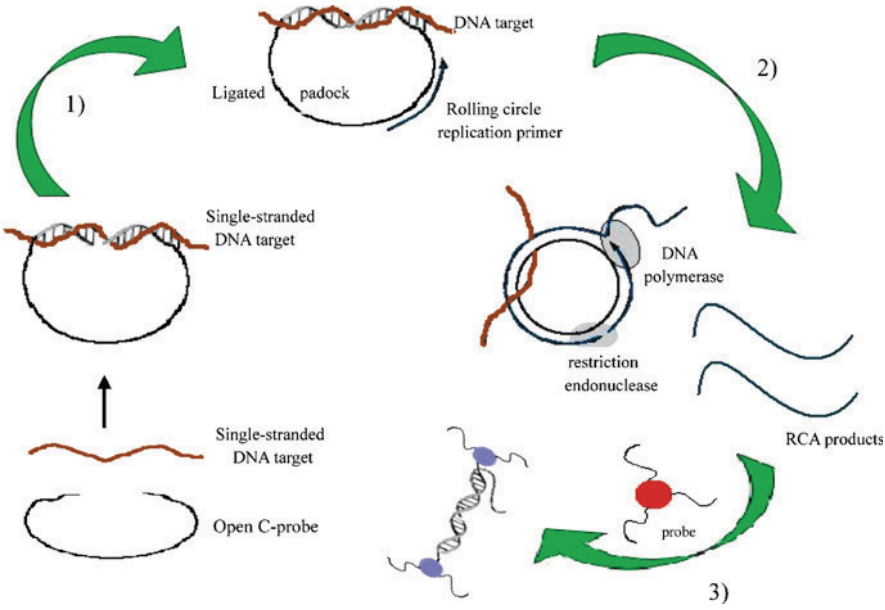

Fig. 2.2 Schematic illustration of the RCA reaction and Au NP assembly-based assay: (**1**) hybridization between padlock probe and target and ligation; (**2**) RCA and digestion; (**3**) colorimetric detection via the assembly of Au NP-tagged DNA probes. Reprinted with permission from Li et al. [28]. © 2010, American Chemical Society

detection of mutant targets even when the ratio of the wild type to the mutant is 10,000:1. The developed RCA-based colorimetric detection scheme has been demonstrated for SNP typing of the thalassemia gene at position 28 in genomic DNA.

A sandwich-type assay for the optical detection of DNA using multicomponent cross-linked Au NP aggregates was reported by Fan (Fig. 2.3) [29]. In their work, a DNA-bridged multi-functional Au NP aggregate, which integrated DNA recognition (detection probe [DP]), signal amplification (enzyme, horseradish peroxidase, HRP), and nonspecific blocking (bovine serum albumin, BSA) section, was employed as the DP. In a typical sensing process, the Au aggregates' DP was brought to the proximity of magnetic particles through the DNA hybridization. Once the magnetic field was added, these sandwich complexes were magnetically separated. As a result, HRP that was confined at the surface of Au aggregates could catalyze the enzyme substrate and generate an optical signal. This assay was employed for the detection of breast cancer–associated BRCA-1 gene. The detection limit was about 1 fM, which was significantly improved compared with the results obtained from individual Au NP-labeled assays.

Figure 2.4 shows a sensitive detection method for adenosine (AD) in human urine by using enhanced-resonance light scattering (RLS) [30]. It is based on the specific recognition and signal amplification of AD aptamer (Apt) coupled with Au NPs via G-quartet–induced NP assembly, which is fabricated by triggering a structure switching of the 30 terminus G-rich sequence and Apt duplex. The RLS signal linearly

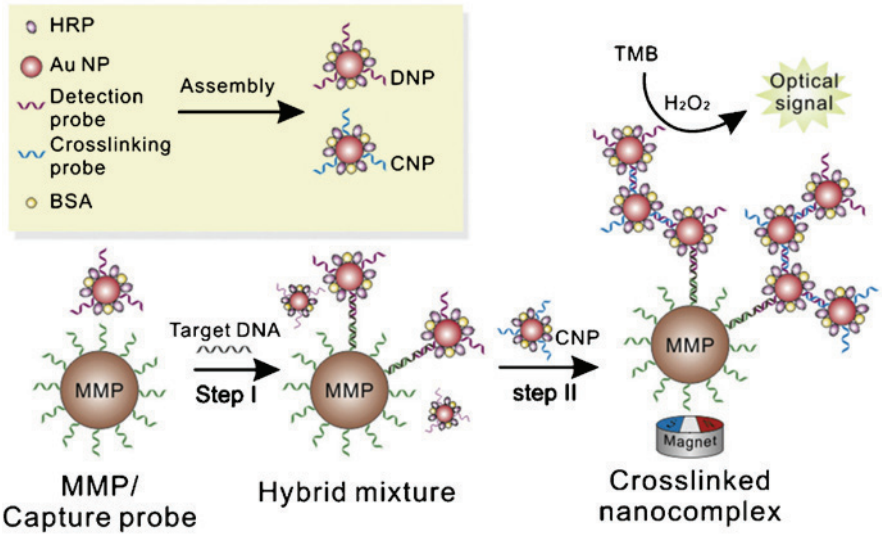

Fig. 2.3 Schematic for the amplified sandwich-type detection assay of the BRCA-1 gene using multifunctional cross-linked Au aggregates and magnetic particles. *Note*: The drawing is not to scale. Reprinted with permission from Li et al. [29]. © 2009, Elsevier

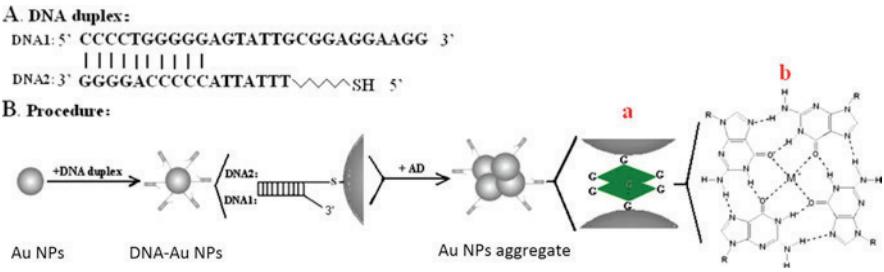

Fig. 2.4 Schematic diagram for analytical principle. (**a**) DNA duplex; (**b**) procedure of Au NPs aggregate. (*a*) G-quartets stacked perpendicularly to the column axis; (*b*) four guanines fold into a G-quadruplex structure by Hoogsteen hydrogen bonds. Reprinted with permission from Zhang et al. [30]. © 2010, Elsevier

correlates with the concentration of AD over the range of 6–115 nM. It has been applied to detect AD in real human urine, and the obtained results are in good agreement with those obtained by the HPLC method. This study illustrates that the combination of the excellent selectivity of Apt with the high sensitivity of the RLS technique provides promising potential for Apt-based small-molecule detection, and may be beneficial in extending the applications of RLS.

Based on Au NP probes, a one-step, washing-free, and amplification-free assay for protein analysis via dynamic light scattering (DLS) has been developed (Fig. 2.5) [31]. The concentration of the target protein is determined by analyzing the level of Au NP

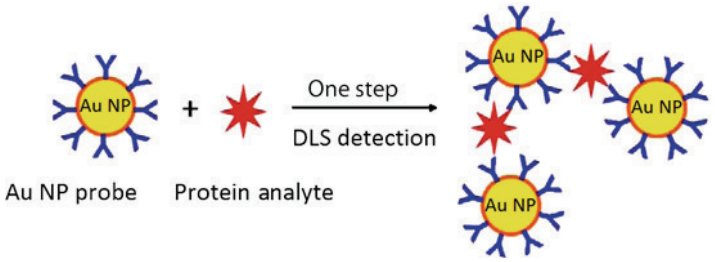

Fig. 2.5 Illustration of a one-step homogeneous biomolecular assay using gold nanoparticle (NP) probes as light-scattering enhancers coupled with dynamic light-scattering detection. Reprinted with permission from Liu and Huo [31]. © 2009, Elsevier

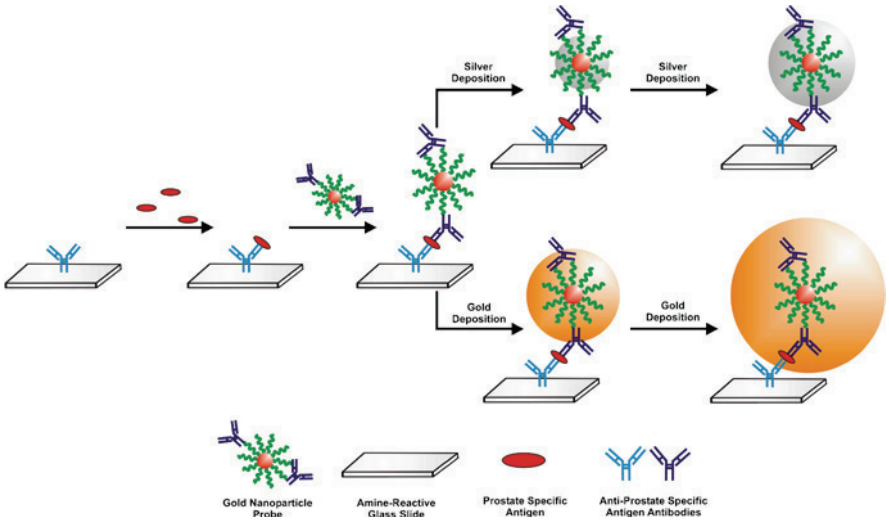

Fig. 2.6 Scanometric immunoassay. Reprinted with permission from Kim et al. [32]. © 2009, American Chemical Society

aggregation caused by antibody–antigen interactions using DLS. The mouse IgG is directly mixed with Au NPs conjugated to goat antimouse IgG. Due to the multiple binding sites of primary mouse IgG by the secondary antibody, mouse IgG causes NP aggregation. Mouse IgG can be detected at a concentration as low as 0.5 ng/mL, and the dynamic range of this assay is between 0.5 and 50 ng/mL. On the other hand, with the use of both mouse IgG and goat antimouse IgG-conjugated Au NPs, this study designs a competitive assay, in which mouse IgG is detected within a dynamic range of 100 ng/mL to 10 μg/mL.

The use of gold development results in greater signal enhancement than the typical silver development, and multiple rounds of metal development have been found to increase the resulting signal compared to one development (Fig. 2.6) [32]. An antibody microarray is fabricated by spotting monoclonal capture antibodies to the surface

of *N*-hydroxysuccinimide-activated glass slides (CodeLink, SurModics). Six spots, all with antibodies for PSA, are used in each assay well. The use of six spots allows statistically significant data to be obtained in each assay. The slides are then passivated with ethanolamine. Probes are prepared by first modifying 13-nm-diameter Au NPs with 3′-propylthiol and 5′-decanoic acid–modified oligonucleotides and then covalently immobilizing antibodies for PSA via carbodiimide coupling. The assay begins by incubating the test solution with PSA at a designated concentration with capture antibodies on the chip (assay buffer: Dulbecco's PBS with 0.1% Tween-20, 0.1% BSA, and 1% poly(acrylic acid)). After that, Au NP probes are incubated with the microarray-bound targets. To increase the light-scattering signal of the immobilized Au NP probes, gold or silver is catalytically deposited on the chip using electroless deposition techniques. Finally, the light scattering is quantified with a Verigene Reader system, which is a device that captures evanescent wave-induced light scattering from the amplified Au NPs. Under these conditions, the assay is capable of detecting 300 aM of PSA in buffer and 3 fM in 10% serum. Additionally, the highly selective detection of three tumor markers at low picomolar concentrations in buffer and 10% serum has been demonstrated. The use of gold deposition may have significant utility in scanometric detection schemes and in broader clinical and research applications.

A homogeneous colorimetric DNA detection by a novel nicking endonuclease-assisted nanoparticle-amplification (NEANA) process has been reported to recognize long single-stranded oligonucleotides with single-base mismatch selectivity and a 100-fold improvement in amplification [33]. A three-component sandwich assay format that included a target DNA (tDNA) and two sets of oligonucleotide-modified NP probes is typically used in conventional homogeneous NP-based colorimetric DNA detection. tDNA serves as a linker strand that triggers particle aggregation and a concomitant color change. The colorimetric detection limit is directly associated with the minimum number of the linkers required to initiate particle aggregation that can be visualized with the naked eye. However, at low linker concentrations (e.g., 10 nM), the aggregation of 14-nm NPs cannot exhibit sharp colorimetric melting transitions. Normally, there are two ways to improve the sensitivities of the colorimetric assay: Enlarge the size of particle probes, or reduce the surface coverages of the oligonucleotide. The former is dominant in sedimentation. To increase the sensitivity of homogeneous NP-based assays, the nicking endonuclease is specifically designed to cleave only the linker strand [34]. As shown in Fig. 2.7, after nicking, the fragments of the linker strand spontaneously dissociate from the tDNA at an elevated temperature. Subsequently, another linker strand hybridizes to the target to continue the strand-scission cycle, which results in the cleavage of a large molar excess of linkers. Upon completion of the strand-scission cycle, two sets of different oligonucleotide-modified gold NPs with sequences complementary to that of the linker strand are added to the solution to detect the presence of a tDNA (Fig. 2.8). If the linker DNA is noncomplementary to the tDNA, particle aggregation will occur. This system offers handling convenience and ultrahigh detection sensitivity and selectivity, and provides additional detection versatility for long-stranded DNA sequences.

Another approach to increase the signal intensity of dye-based assays is metal-enhanced fluorescence (MEF) [35–38]. MEF is the result of interactions between

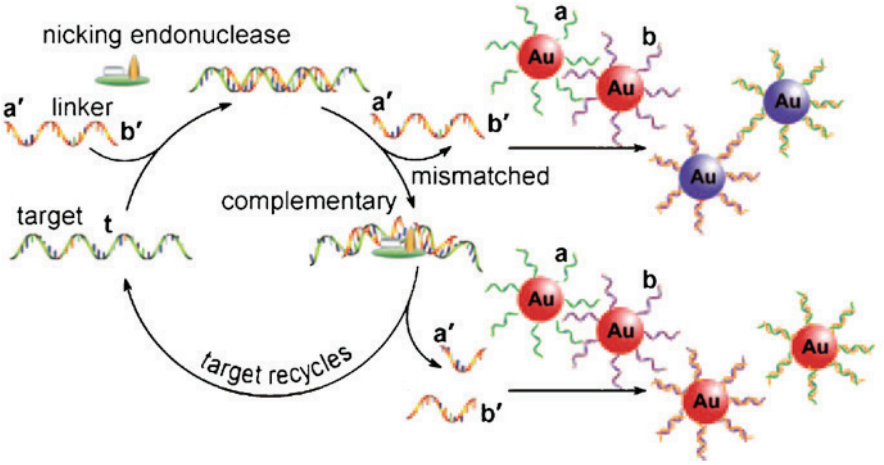

Fig. 2.7 Nicking endonuclease-assisted NP amplification for target DNA detection. Reprinted with permission from Xu et al. [34]. © 2009, Wiley

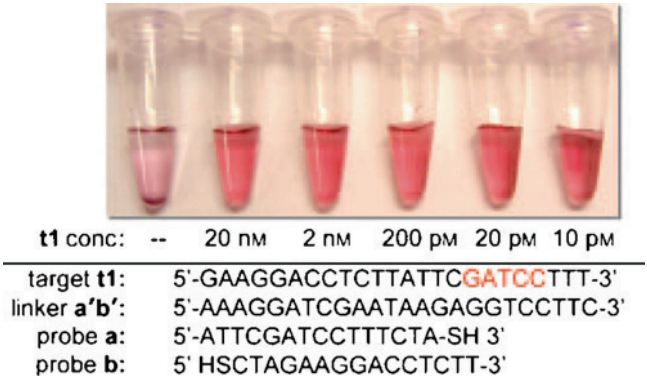

Fig. 2.8 Photograph showing colorimetric responses of a NEANA detection system. The labeled concentrations (20 nM, 2 nM, 200 pM, 20 pM, and 10 pM) are the calculated final target concentrations in solutions. The NEase recognition site of the target is highlighted in red. Reprinted with permission from Xu et al. [34]. © 2009, Wiley

fluorophores and surface plasmons in metallic nanostructures, most typically in Ag [39, 40] and Au [41, 42]. Enhanced emissions can be obtained as a result of an amplification of the incident electric field, which effectively increases the fluorophore's absorption cross-section, or by an acceleration of the radiative decay rate [43–47]. These desirable effects need to counterbalance possible emission suppression by energy transfer to the metallic surfaces [48–50]. Nevertheless, differences in spatial and orientational dependencies between amplification and quenching mechanisms allow one to find appropriate emitter-surface environments and organizations where an improved performance is obtained [37]. The examples include MEF-based assays for DNA [51], RNA [52], and immunological applications [53].

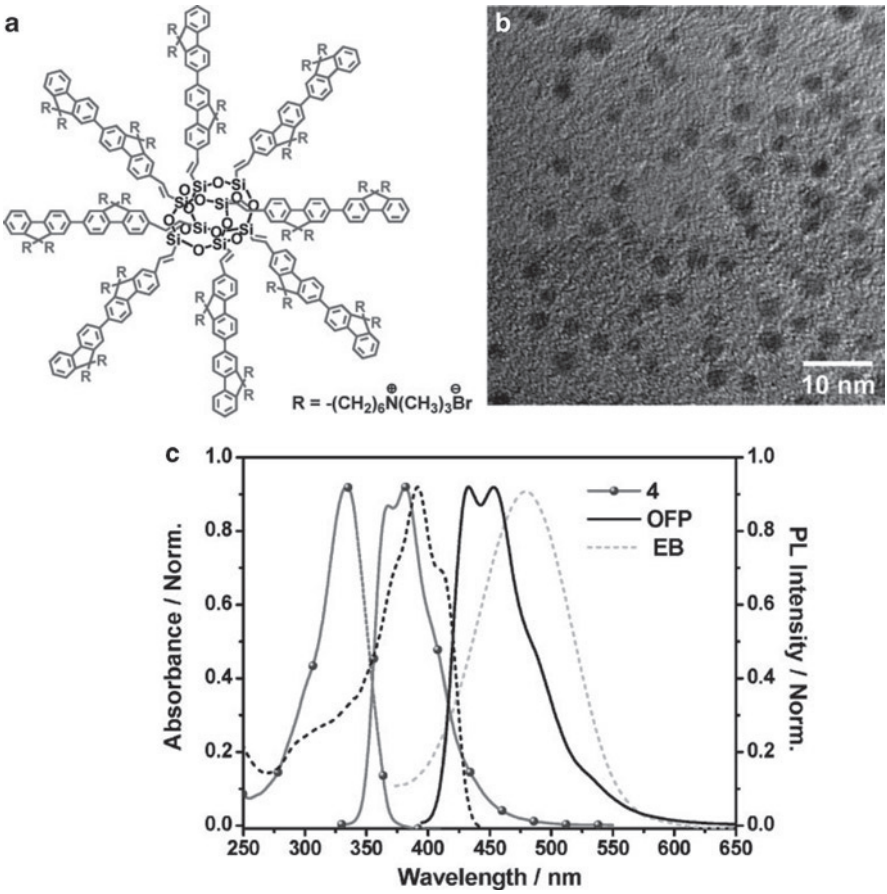

Fig. 2.9 (**a**) Chemical structure of OFP; (**b**) HR-TEM image of OFP; (**c**) normalized UV–vis absorption spectra of the arm 4, OFP, and EB (*dashed lines*), and PL spectra of 4 and OFP (*solid lines*) in water. Reprinted with permission from Pu et al. [54]. © 2010, Wiley

Using hybrid nanomaterials as the signal amplifiers, Pu et al. provided a new way to improve the performance of fluorescence technologies for biological imaging through a fluorescence resonance energy transfer (FRET) approach [54]. From the materials viewpoint, the emission wavelength, charge nature, and diameter of polyhedral oligomeric silsesquioxane (POSS)-based fluorescent NPs can be easily adjusted through chemical modification of fluorescent arms so as to fulfill the different requirements of specific applications. In terms of materials applications, the high quantum yields and good signal amplification capability of POSS-based molecules allow high-quality biological imaging even with a small amount of indicator dyes, consequently avoiding the side effect of elevated dye concentrations. In view of their aggregation-inhabited nanostructures and environment-resistant fluorescence, POSS-based nanomaterials are also appropriate for signal amplification in various biological assays, such as DNA and protein microarrays (Fig. 2.9).

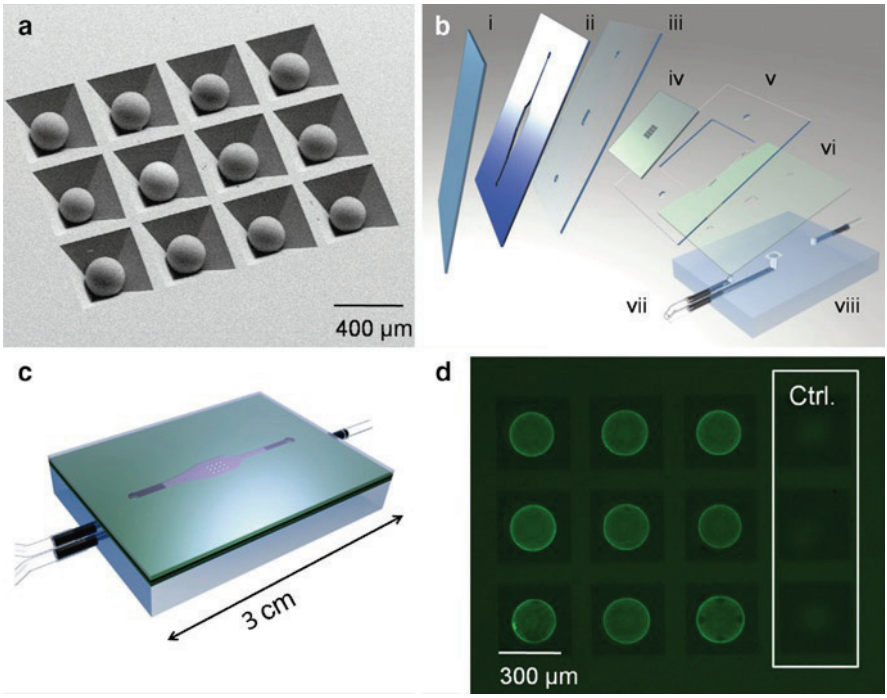

Fig. 2.10 (**a**) SEM photomicrograph of beads in anisotropically etched silicon chip. (**b**) Chip (iv) is fitted between double-sided adhesive layer (ii) and cover slip (i) with laminate layers (iii, v, vi) included to direct fluid flow through the PMMA base (viii) and inlet and outlet ports (vii). (**c**) Sealed LOC assembly. (**d**) Fluorescent image of beads after immunoassay, including negative controls as imaged with 1 s of CCD camera integration (exposure) time. Reprinted with permission from Jokerst et al. [55]. © 2009, Elsevier

2.2.2 Semiconductor Nanoparticle-Based Amplification

Similarly, semiconductor NPs exhibit size-dependent tunable absorbance and fluorescence. The high-fluorescence quantum yields, photostability, and tunable fluorescence bands of semiconductor NPs have attracted substantial research efforts directed toward the use of semiconductor NPs as fluorescence labels for biorecognition processes.

With the integration of semiconductor NP quantum dots (QDs) into a modular, Jokerst et al., designed a microfluidic biosensor for the multiplexed quantitation of three important cancer markers: carcinoembryonic antigen (CEA), cancer antigen 125 (CA125), and Her-2/Neu (C-erbB-2) (Fig. 2.10) [55]. Nanobiochips that employed a fluorescence transduction signal with a QD-labeled detecting antibody were used in combination with antigen capture by a microporous agarose bead array supported within a microfluidic ensemble so as to complete the sandwich-type immunoassay. The utilization of QD probes in this miniaturized biosensor format

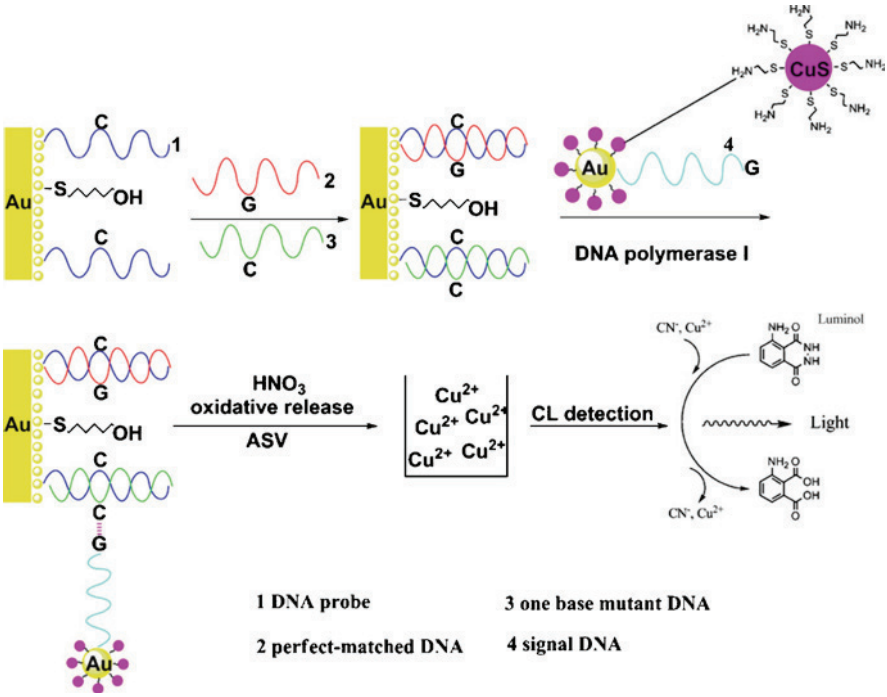

Fig. 2.11 Schematic of CL SNP quantitative assay based on Au and CuS NP probe and one-step DNA hybridization reaction. Reprinted with permission from Ding et al. [56]. © 2010, Elsevier

resulted in a 30-fold signal amplification relative to that of standard molecular fluorophores as well as reduced observed limits of detection by nearly two orders of magnitude (0.02 ng/mL CEA; 0.11 pM CEA) relative to enzyme-linked immunosorbent assay (ELISA). Assay validation studies indicated that measurements by the nanobiochip system correlated to standard methods at $R^2 = 0.94$ and 0.95 for saliva and serum, respectively. This integrated nanobiochip assay system, in tandem with next-generation fluorophores, would be a sensitive, multiplexed tool for important diagnostic and prognostic applications.

2.2.3 Nanoparticle-Amplified Chemiluminescence and Electrogenerated Chemiluminescence Assay

The functionalized NPs have been used to enhance the chemiluminescence (CL) or electrogenerated chemiluminescence (ECL) intensity. An ultrasensitive CL method based on the Au NP' amplification for the quantitative detection of SNPs in genomic DNA has been accomplished by the DNA polymerase I (Klenow fragment)-induced coupling of the nucleotide-modified NP probe to the mutant sites of duplex DNA under the Watson–Crick base-pairing rule [56]. As shown in Fig. 2.11, Au NPs

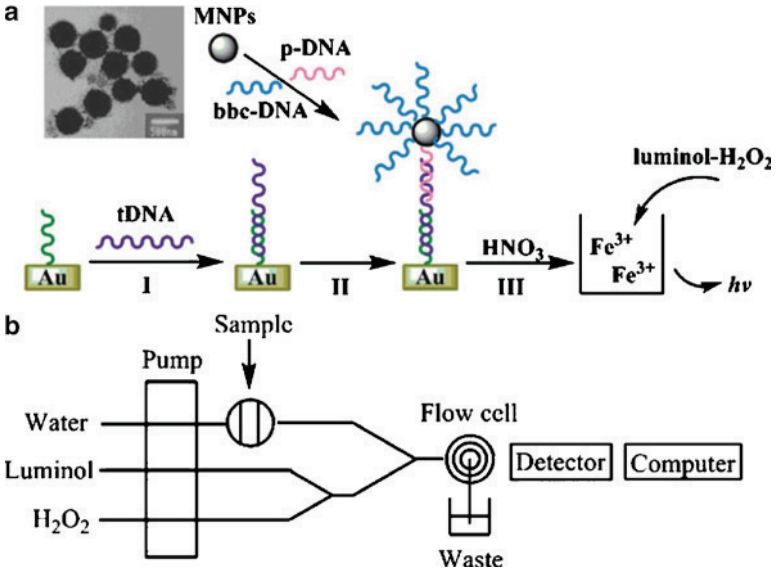

Fig. 2.12 (**a**) Schematic representation of the CL detection of DNA hybridization based on bio-barcode-functionalized magnetic nanoparticle labels (bbcMNPs) (*upper part*: carboxyl-coated MNPs (carboxyl-MNPs) are functionalized with amino-modified probe DNA (amino-pDNA) and amino-modified bio-barcode DNA (amino-bbcDNA), fabricating bbc-p-DNA-MNPs). (**b**) Schematic diagram of the FI-CL detection system for the determination of Fe^{3+}. Reprinted with permission from Bi et al. [58]. © 2009, Royal Society of Chemistry

are first electrodeposited on the surface of the Au electrode for DNA probe immobilization, followed by the hybridization between the DNA probe and the mixture of the single-base-mismatched tDNA and complementary tDNA. Au NP probes modified with CuS NPs and a base (guanine, G) that is complementary to the mutation site (cytosine, C) are coupled to the formed duplex DNA in the presence of DNA polymerase. CuS NPs and Au NPs are linked by an amidization reaction between mercaptoacetic acid on the surface of Au NPs and aminoethanethiol on the surface of CuS NPs. The base G and the Au NP are linked by DNA with a sequence of 5′-SH-$(CH_2)_6$-ATG TCC CTC AGA CCC TTT-$(CH_2)_6$-NH_2-3′. The amount of the SNPs is monitored by the CL intensity of luminol-CN^--Cu^{2+} after the cupric ions are dissolved from the hybrid (Fig. 2.11). A preconcentration processing of cupric ions is performed by anodic stripping voltammetric (ASV) technology to improve the sensitivity of the method. The mechanism of the luminol–CN^-–Cu^{2+} CL system to produce CL signal is based on coupling the complex-formation reaction of cupric ions and cyanide with the CL reaction of luminal and $Cu(CN)_4^{2-}$, which has a high oxidation potential. As a single Au NP can be loaded with 77 CuS NPs, the incorporation of Au NPs significantly enhances the sensitivity. Moreover, the preconcentration processing of cupric ions can further increase the sensitivity about tenfold. As a result of these two combined effects, this method could detect as low as 19 aM SNPs, and the linear range for SNPs was from 8.0×10^{-17} to 1.0×10^{-14} M. Based on this

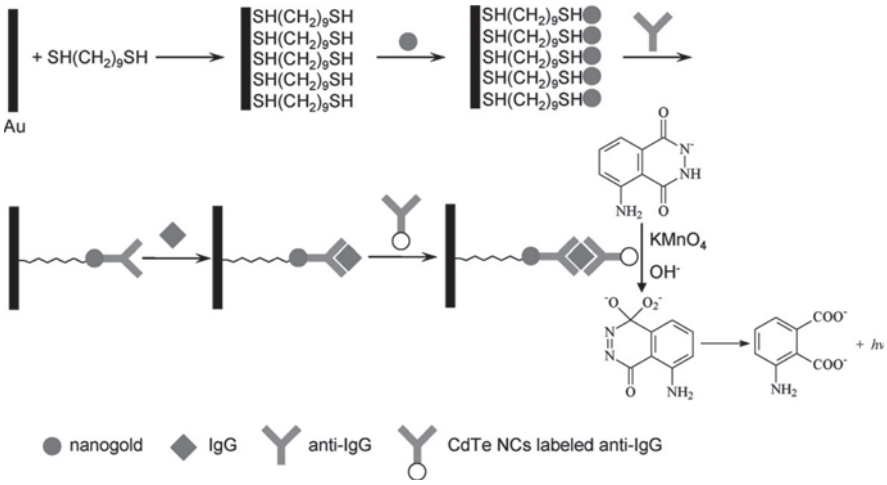

Fig. 2.13 CL immunoassay of IgG using CdTe QDs as label. Reprinted with permission from Wang et al. [59]. © 2009, Elsevier

strategy, Zhang's group also demonstrated a dual amplification with thrombin-labeled PbS NPs and thiocyanuric acid–gold NP network for DNA detection [57].

On the other hand, Zhang's group developed an FI-CL detection platform of DNA hybridization based on bio-barcode-functionalized magnetic nanoparticle (MNPs) labels [58]. As shown in Fig. 2.12, thiolated cDNA was assembled on the Au electrode surface via sulfur–gold affinity, and bbcDNA and pDNA were labeled with carboxyl-modified MNPs on the 5′-NH_2 end, both of which flanked the tDNA, resulting in the fabrication of a sandwich-type detection protocol. Compared with single DNA probe strands, MNPs containing pDNA and bbcDNA could avoid cross-reaction and improve the detection sensitivity of tDNA. Once the ferric ions were dissolved from the hybrids, the large amount of released ferric ions could be sensitively determined by the luminol–H_2O_2–Fe^{3+} CL reaction system and generated a strong CL signal. The CL intensity was proportional to the amount of tDNA based on the concentration of dissolved ferric ions. A detection limit of 0.32 fM could be achieved without any preconcentration process.

Li and his coworkers [59] found that mixing CdTe QDs with luminol in the presence of $KMnO_4$ could induce a greatly sensitized effect on CL emission. The CL spectra displayed that there was only one peak emission, around 425 nm, for the luminol–CdTe QD–$KMnO_4$ system when scanned from 300 to 700 nm, which was in agreement with that of the luminol–$KMnO_4$ system. Moreover, the CL intensity of the luminol–$KMnO_4$–CdTe QD system was obviously stronger than that of the luminol–$KMnO_4$ system, indicating the sensitized effect of CdTe QDs on the luminol–$KMnO_4$ CL reaction due to the accelerated luminol CL induced by the oxidized species of CdTe QDs. Based on this finding, using thioglycolic acid (TGA)-capped CdTe QDs as a label and IgG as a model analyte, Li's group designed a CL immunoassay (CLIA) protocol for IgG content detection (Figs. 2.13 and 2.14). Overall, the studies strongly demonstrated the possibility that QDs induced CL for more practical applications.

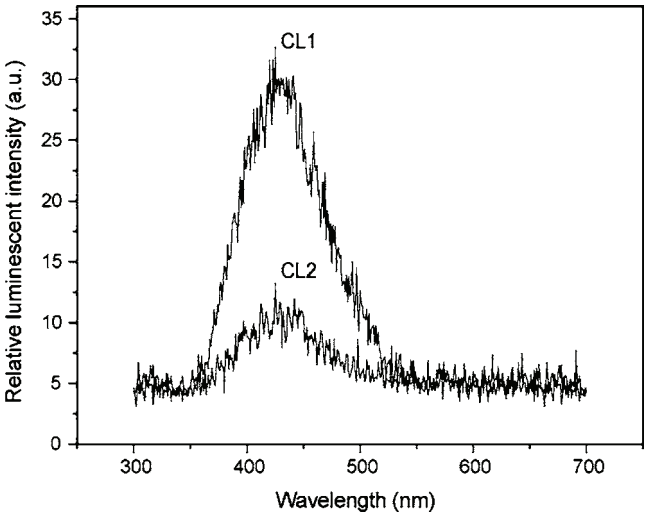

Fig. 2.14 CL spectra of luminol–$KMnO_4$ in the presence of CdTe QDs (CL1) and luminol–$KMnO_4$ in the absence of CdTe QDs (CL2). Conditions: luminol, 1×10^{-5} M (in 0.01 M NaOH); $KMnO_4$, 1×10^{-5} M; CdTe QDs, 1×10^{-3} M. Reprinted with permission from Wang et al. [59]. © 2009, Elsevier

Zhu's group [60] indicated that the ECL of CdSe QDs could be greatly enhanced by combining carbon nanotubes (CNTs) and poly (diallyldimethylammonium chloride) (PDDA) in CdSe QD film. Based on this phenomenon, they developed a sensitive ECL immunosensor for the detection of human IgG (Ag). The fabrication procedures for CdSe QD–CNT conjugates and the ECL immunosensor were shown in Fig. 2.15. Where PDDA as a binding linker was conjugated to the CdSe QD–CNT composite film on the electrode, the ECL signal was significantly enhanced. Subsequently, Au NPs assembled onto the CdSe QD–CNT/PDDA–modified electrode amplified the ECL signal once again. After antibody (Ab) was immobilized onto the electrode through Au NPs, the ECL immunosensor was fabricated. The principle of ECL detection for target Ag was based on the increment of steric hindrance after immunoreaction, which resulted in a decrease in the ECL intensity (Fig. 2.16). The Ag concentration was determined in the linear range of 0.002–500 ng/L, with a detection limit of 0.6 pg/mL.

When nanoporous gold leaf (NPGL) electrodes are used, the sensitivity of the ECL assay can be remarkably increased due to ultrathin nanopores. Based on this phenomenon, Hu et al. [61] developed a sensitive ECL DNA assay (Fig. 2.17). In this assay, tDNA was hybridized with capture DNA (cDNA) bound on the NPGL electrode, which was fabricated by conjugating amino-modified cDNA to TGA modified at the activated NPGL electrode. Following that, amino-modified probe DNA was hybridized with the tDNA, yielding

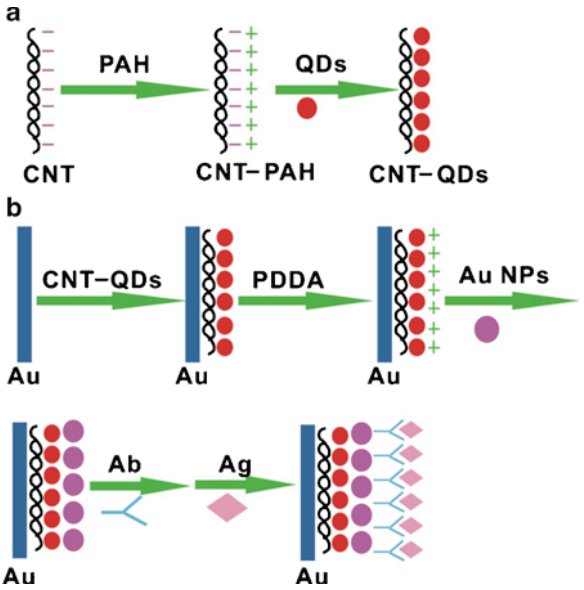

Fig. 2.15 The fabrication procedures for (**a**) CdSe QDs–CNTs conjugates and (**b**) the ECL immunosensor. Reprinted with permission from Jie et al. [60]. © 2009, Elsevier

sandwich hybrids on the NPGL electrode. Then, mercaptopropionic acid–capped CdTe QDs were labeled to the amino group end of the sandwich hybrids. Finally, in the presence of $S_2O_8^{2-}$ as coreactant, the ECL emission of the QD-labeled DNA hybrids on the NPGL electrode was measured by scanning the potential from 0 to −2 V to record the curve of ECL intensity vs. potential. The maximum ECL intensity on the curve was proportional to the tDNA concentration, with a linear range of 5×10^{-15}–1×10^{-11} mol/L (Fig. 2.18).

The broad-spectrum expression of telomerase in most malignancies makes it a promising target as a cancer diagnostic and prognostic tool. Conventional PCR-based telomerase activity assay is highly sensitive but susceptible to amplification-related errors. The ECL detection method for telomerase activity is accomplished by the hybridization of ECL nanoprobes to telomerase reaction products, the subsequent capture by magnetic beads (MBs), and in situ measurement of the light signal from ECL nanoprobes [62]. The ECL intensity directly reflects the quantity of telomerase reaction products, which corresponds to the telomerase activity. The high sensitivity afforded by the current MB and NP-based ECL detection platform allows the measurement of telomerase activity from as little as 500 cultured cancer cells in crude cell extracts without the PCR amplification of telomerase reaction products. In addition, a comparative study of the ECL nanoprobe and linear telomere antisense ECL probe has been executed. By using the ECL nanoprobe, one obtains about a 100-fold elevation in sensitivity. This method is ideal for telomerase activity analysis due to its reliability and high sensitivity.

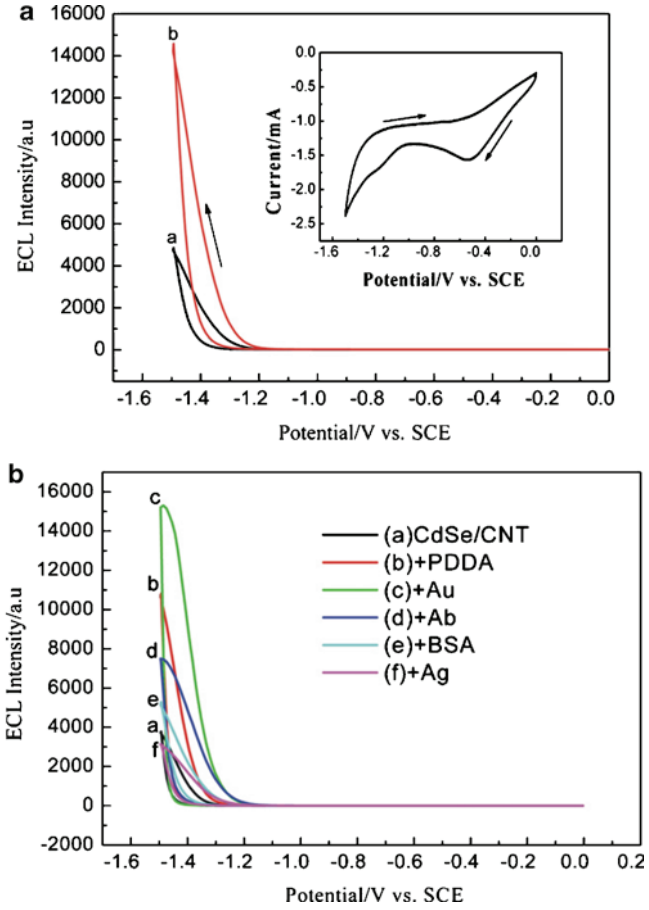

Fig. 2.16 ECL–potential curves of (**a**) CdSe QDs–CNTs; (**b**) (*a*)+PDDA; (*c*) (*b*)+GNPs; (*d*) (*c*)+Ab; (*e*) (*d*)+BSA; and (*f*) (*e*)+Ag-modified Au electrodes in 0.1 M PBS (pH 7.4) containing 0.1 M KCl and 0.1 M $K_2S_2O_8$. Scan rate: 100 mV/s. Reprinted with permission from Jie et al. [60]. © 2009, Elsevier

2.3 Nanoparticle-Amplified Electrochemical Detection

2.3.1 Enhanced Conductivity with Nanoparticles

The formation of conductive domains, as a result of biomolecular interactions of proteins and the enlargement of gold NP tags, provides an attractive route for electrochemical transduction of biorecognition events. For example, based on NP-induced changes in the conductivity across a microelectrode gap, Velev and Kaler [63] developed conductivity immunoassays of proteins in connection to antibody-functionalized latex spheres placed between two microelectrodes.

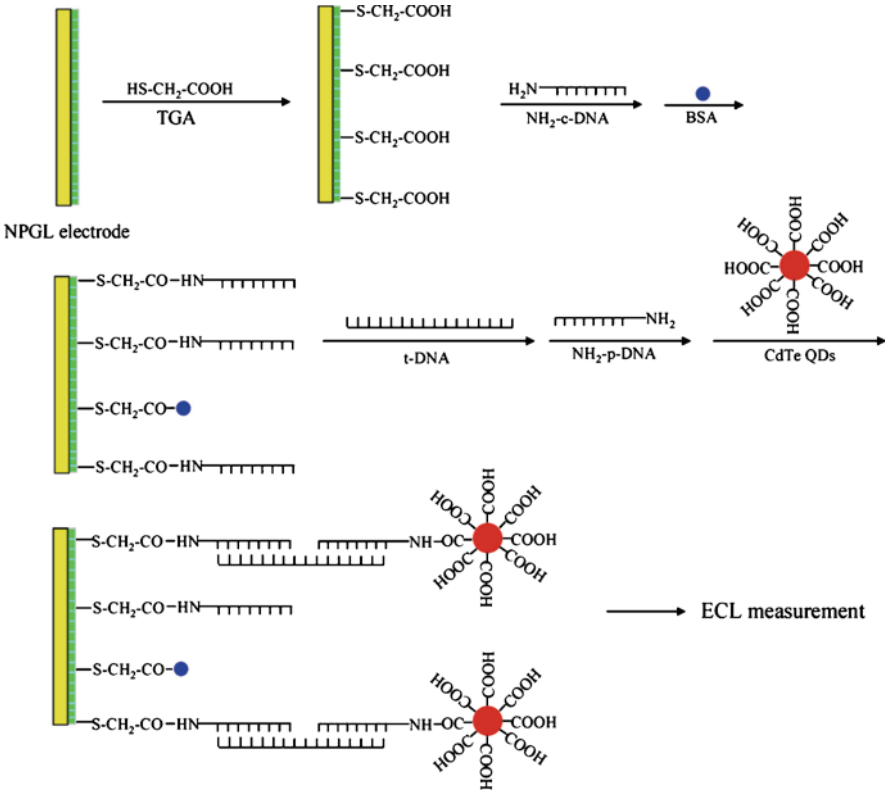

Fig. 2.17 Schematic representation of the process of DNA determination. Reprinted with permission from Hu et al. [61]. © 2010, Elsevier

Sandwich immunoassay led to the binding of a secondary gold-labeled antibody, followed by the catalytic deposition of a silver layer to "bridge" the two electrodes. Such a formation of conductive paths across interdigitated electrodes led to a measurable conductivity signal and enabled the ultrasensitive detection of human IgG down to the 2×10^{-13} M level. This method holds promise for creating miniaturized on-chip protein arrays. Analogous measurements of DNA hybridization were also reported by Mirkin's group [64].

The extensive knowledge in the preparation of metal and semiconductor NPs functionalized with biomaterials suggests that the unique catalytic or photoelectrochemical properties of the NPs can be used to develop electrochemical and photoelectrochemical biosensors [63]. For example, the catalytic electroless deposition of metals on NP-hybrid labels can be used to generate conductive domains on functionalized or patterned surfaces, and the conductivity properties of the systems then transduce the biosensing processes.

Silver-enhanced labeling is frequently employed in immunochromatographic assays to improve the sensitivity of detecting pathogens. For example, Liu et al. [65]

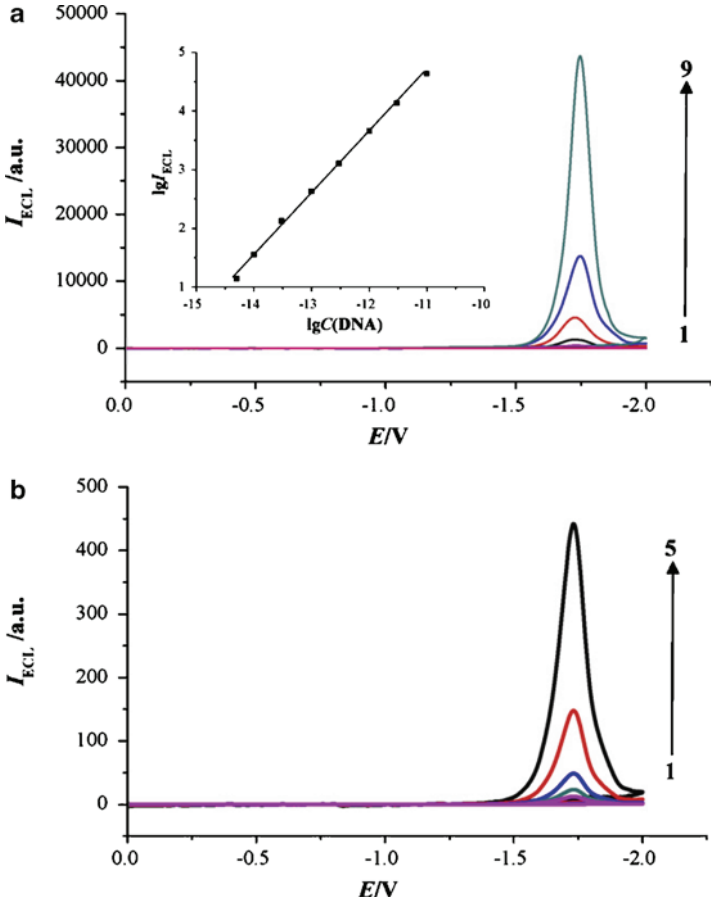

Fig. 2.18 (**a**) IECL–E curves of CdTe QD-labeled DNA hybrids immobilized on an NPGL electrode in PB (pH 7.4) containing 0.1 mol/L $K_2S_2O_8$ and 0.1 mol/L KNO_3 for different t-DNA concentrations (10^{-15} mol/L): (1) 0, (2) 5.0, (3) 10, (4) 30, (5) 100, (6) 500, (7) 1,000, (8) 2,000, (9) 4,000, (10) 6,000, (11) 8,000, and (12) 10,000. (**b**) Magnification of the IECL–E curves indicated in (1–5). *Inset*: Relationship between I_{ECL} and t-DNA concentration. Reprinted with permission from Hu et al. [61]. © 2010, Elsevier

applied a silver enhancement technique for biomolecular signal amplification in a gold NP–based conductimetric biochip. The response of the silver-enhanced biochip comprised two distinct regions: (1) a subthreshold region, where conduction occurred due to electron hopping between silver islands and the electrolyte; and (2) an above-threshold region, where the conduction was due to a direct flow of electrons. These two regions were characterized by different conduction slopes. Results from fabricated prototypes showed a dynamic range of more than 40 dB and with a detection limit of 240 pg/mL.

2.3.2 *Detection of Nanoparticle Label with Stripping Voltammetry*

Powerful NP-based electrochemical DNA hybridization assays have been developed using Au and Ag metal tracers [66–69]. Such protocols rely on capturing the gold [66, 67] or silver [68] NPs to the hybridized target and use ASV to measuring the metal tracer electrochemically. The probe or target immobilization is accomplished directly on a carbon or indium-tin oxide (ITO) electrode [70, 71]. Picomolar and subnanomolar levels of the DNA target can be detected. For example, an electrochemical method is employed for the Au NP–based quantitative detection of the 406-base human cytomegalovirus DNA sequence (HCMV DNA) [67]. The HCMV DNA is immobilized on a microwell surface and hybridizes with the complementary oligonucleotide-modified Au NP. The resulting surface-immobilized Au NP double-stranded assembly is treated with HBr/Br_2 for oxidative dissolution of the gold particles. The solubilized Au^{3+} ions are then electrochemically reduced and accumulated on the electrode and subsequently determined by ASV using a sandwich-type screen-printed microband electrode (SPMBE). As the nonlinear mass transport of the ions and the release of a large number of Au^{3+} ions upon the dissolution of the particle associate with a single recognition event, this method enables detection of the HCMV DNA as low as 5×10^{-12} M. Further sensitivity enhancements can be obtained by catalytic enlargement of the gold tracer in connection to NP-promoted precipitation of gold [66] or silver [72, 73]. Combining the metal particle tags with the electrochemical stripping analysis paved the way to subpicomolar detection limits.

Another example is presented as an ultrasensitive technique for the electrochemical detection of the mutated *BRAF* gene associated with papillary thyroid carcinomas (PTC) [74]. The biotinylated 30-nucleotide probe DNA is immobilized in a streptavidin-modified 96-well microtiter plate, and the free active sites of the streptavidin are blocked by biotinylated BSA. The biotinylated tDNA is then added and allowed to hybridize with the immobilized probe DNA. Subsequently, streptavidin-labeled gold NPs are added, and a NP enlargement process is performed using gold ion solution and formaldehyde reductant. The gold NPs are then dissolved in bromide, and the detection process of DNA hybridization is performed using a square-wave stripping voltammetry (SWSV) technique. The coefficient of determination (R^2) of the semilog plot of the SWSV response current against the tDNA concentration (0.52–1,300 aM) is 0.9982. The detection limit is 0.35 aM (based on a signal-to-noise ratio of 3:1). This value is approximately three orders of magnitude lower than that obtained using a similar method without the gold amplification process.

Dequaire et al. [75] demonstrated an electrochemical metal immunoassay based on stripping voltammetric detection of the colloidal gold label. Such a heterogeneous sandwich immunoassay involved capture of the gold-tagged secondary antibody, followed by acid dissolution and anodic-stripping electrochemical measurement of the solubilized metal tracer. This protocol could detect the target IgG protein down to the 3-pM level using a 35-mL sample volume. Such a high sensitivity competed

favorably with colorimetric ELISA assays. This study also indicated that labeling the antibody with gold NPs had no apparent effect on their interaction with their antigen. Further enhancements to sensitivity could be achieved by the cyclic accumulation of gold NPs [76] or the catalytic deposition of metals on core gold NP tags [77, 78].

Recent activities have demonstrated that inorganic nanocrystals offer an electrodiverse population of electrical tags for multiplexed bioanalysis. For example, Wang's group used encoding NPs (cadmium sulfide, zinc sulfide, copper sulfide, and lead sulfide) to the multiplexed detection of DNA targets [79], SNPs [80], and antigens [81]. The multitarget electrical detection capability was coupled to the amplification feature of electrochemical stripping transduction (to yield fM detection limits) and with an efficient magnetic separation (to minimize nonspecific adsorption effects). Each biorecognition event yielded a distinct voltammetric peak, whose position and size reflected the identity and level of the corresponding target. Recently, Wang's group designed a QD/aptamer-based ultrasensitive electrochemical biosensor to detect multiple protein targets [82]. As shown in Fig. 2.19, the protocol was based on a simple single-step displacement assay involving the coimmobilization of several thiolated aptamers, along with binding of the corresponding QD-tagged proteins on a gold surface (a), addition of the protein sample (b), and monitoring of the displacement through electrochemical detection of the remaining nanocrystals (c). Such an electronic transduction of aptamer–protein interactions was extremely attractive for meeting the low-power, size, and cost requirements of decentralized diagnostic systems. A detection limit of 20 ng/L (0.5 pM) was obtained by this biosensor, which was 3–4 orders of magnitude lower than those (1–6.4 nM) obtained with other advanced aptamer biosensors.

With the use of the RCA technique, a cascade signal amplification strategy was proposed for detection of the protein target at an ultralow concentration [83]. In this assay, the ultrasensitive detection was achieved by combining the RCA technique with oligonucleotide-functionalized QDs, multiplex binding of the biotin–streptavidin system, and ASV measurement. As shown in Fig. 2.20, the RCA product containing tandem-repeat sequences could serve as an excellent template for the periodic assembly of QDs, which present per protein recognition event to numerous QD tags for electrochemical readout. Both the RCA and the multiplex binding system showed remarkable amplification efficiency, with very little nonspecific adsorption and low background signal (Fig. 2.21). With human vascular endothelial growth factor (VEGF) as a model protein, the designed strategy could quantitatively detect protein down to 16 molecules in a 100-μL sample with a linear calibration range from 1 aM to 1 pM and was amenable to quantification of the protein target in complex biological matrices. The proposed cascade signal-amplification strategy seems to be a powerful tool for proteomics research and clinical diagnostics.

2.3.3 Nanoparticle-Enhanced Impedance Signal

Due to the electrochemical properties of Au NPs, they have been used as signal amplifiers in many electrochemical DNA biosensors. Wang et al. [84] demonstrated

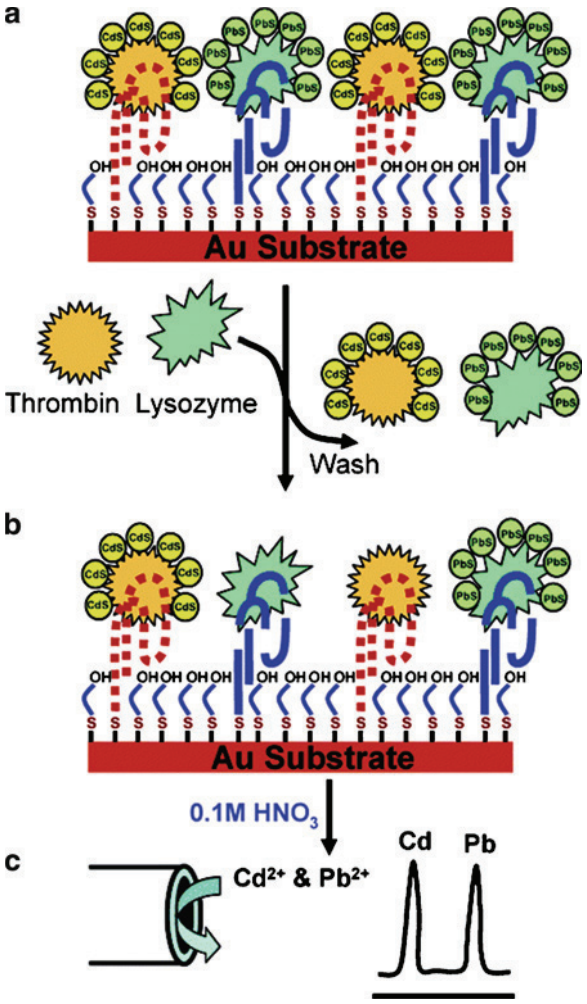

Fig. 2.19 Operation of the aptamer/quantum-dot-based dual-analyte biosensor, involving displacement of the tagged proteins by the target analytes: (**a**) mixed monolayer of thiolated aptamers on the gold substrate with the bound protein–QD conjugates; (**b**) sample addition and displacement of the tagged proteins; (**c**) dissolution of the remaining captured nanocrystals followed by their electrochemical-stripping detection at a coated glassy carbon electrode. Reprinted with permission from Hansen et al. [82]. © 2006, American Chemical Society

that Au NPs could amplify the electrochemical impedance and capacitance signals for the model fluorescein/antifluorescein system. Following the immobilization of fluorescein onto Au through the formation of a self-assembled monolayer, goat anti-fluorescein conjugated with 10-nm Au NPs was introduced into the system. This resulted in an increase of 400 nF/cm^2 in the capacitance, whereas no change could be observed for goat antifluorescein without the Au NP conjugate. This allowed the construction of high-sensitivity electrochemical impedance biosensors at a single low frequency, where the signal was sensitive to the interfacial Rct.

The impedance detection of CEA, a glycoprotein involved in cell adhesion produced only during fetal development, was recently reported [85]. The CEA antibody was first bound through its surface amino groups to glutathione-modified Au NPs of 15–1.5-nm diameter by amide-bond formation using *N*-(3-dimethylaminopropyl)-*N*′-ethylcarbodiimide hydrochloride (EDC) and *N*-hydroxysulfylsuccinimide sodium

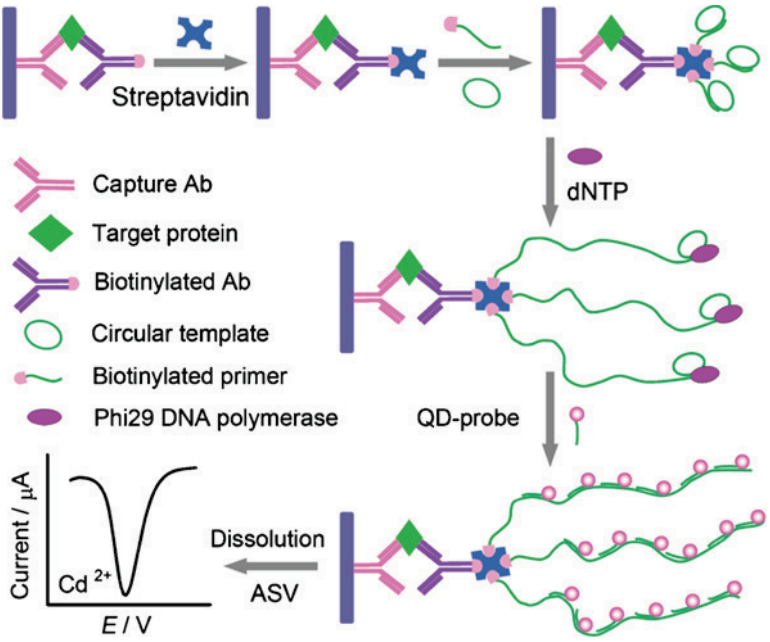

Fig. 2.20 Schematic representation of the cascade signal-amplification strategy for protein detection. Reprinted with permission from Cheng et al. [83]. © 2010, American Chemical Society

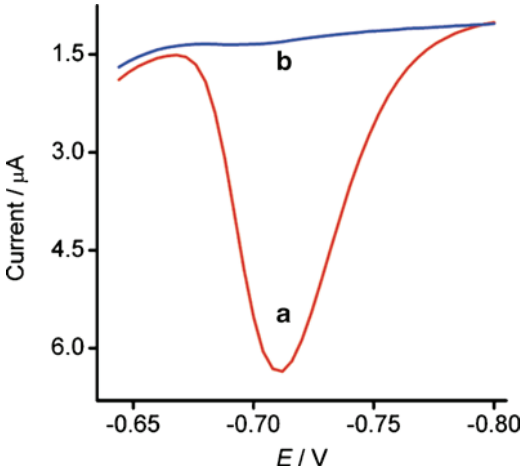

Fig. 2.21 Anodic stripping voltammograms of cadmic cation responding to 1 fM of VEGF (*a*) with and (*b*) without RCA. Reprinted with permission from Cheng et al. [83]. © 2010, American Chemical Society

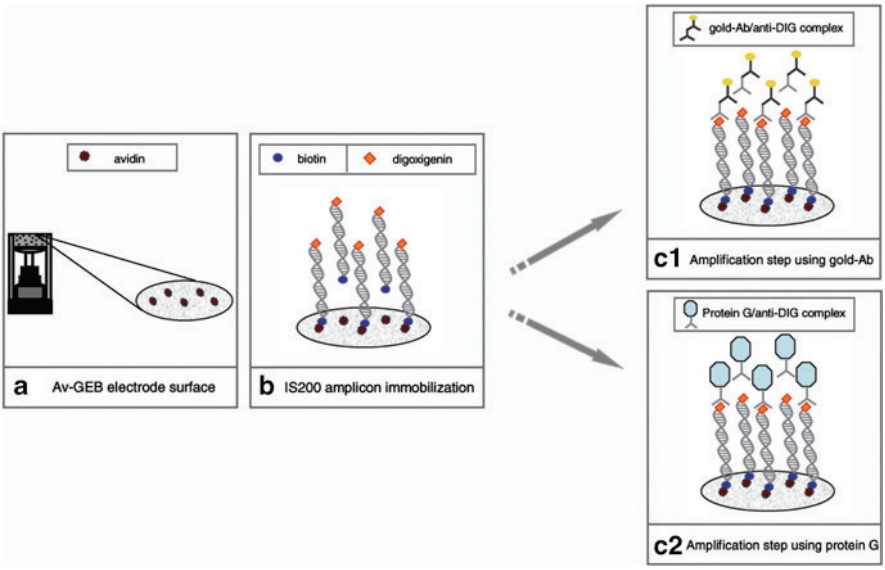

Fig. 2.22 Schematic representation of experimental protocol. (**a**) Representation of the avidin-modified electrode and its surface; (**b**) immobilization of double-labeled IS200 amplicon on the electrode surface through the formation of the biotin–avidin complex; (**c1**) addition of gold-Ab/anti-DIG complex; (**c2**) addition of Protein G. Reprinted with permission from Bonanni et al. [86]. © 2009, Royal Society of Chemistry

salt (NHSS). The sensing interface was formed by copolymerizing a mixture of *o*-aminophenol and the Au-NP-conjugated CEA antibodies. The R_{ct} increased 6.3×10^5 Ω on the sensing interface with Au NPs, while an increase of only 0.59×10^5 Ω on the sensing interface without Au NPs was observed.

Double-tagged DNA coming from the PCR amplification of a *Salmonella* spp. sample has been detected by an electrochemical impedimetric genosensor based on avidin bulk-modified graphite-epoxy biocomposite (Av-GEB) [86]. As shown in Fig. 2.22, the double-tagging PCR strategy provides the amplicon with both biotin and digoxigenin (DIG) moieties. The immobilization of the double-tagged DNA is based on its biotin moiety, while the DIG label is used for signal amplification. Impedance spectra are recorded to detect the change in interfacial charge-transfer resistance, experimented by the redox marker ferri-/ferro-cyanide after the avidin–biotin fixation of the sample DNA onto the electrode surface. A further step in the genosensing strategy is the amplification of impedimetric signal by the use of an enhancing procedure. The latter is based on the reaction of the DIG moiety belonging to the amplicon with an anti-DIG antibody from mouse. Two different secondary enhancing steps, based on gold NP–labeled antimouse IgG or on Protein G, are performed and compared to improve the assay sensitivity.

A renewable, site-selective immobilization platform of microelectrode array (MEA) for multiplexed immunoassays has been developed using pencil graphite

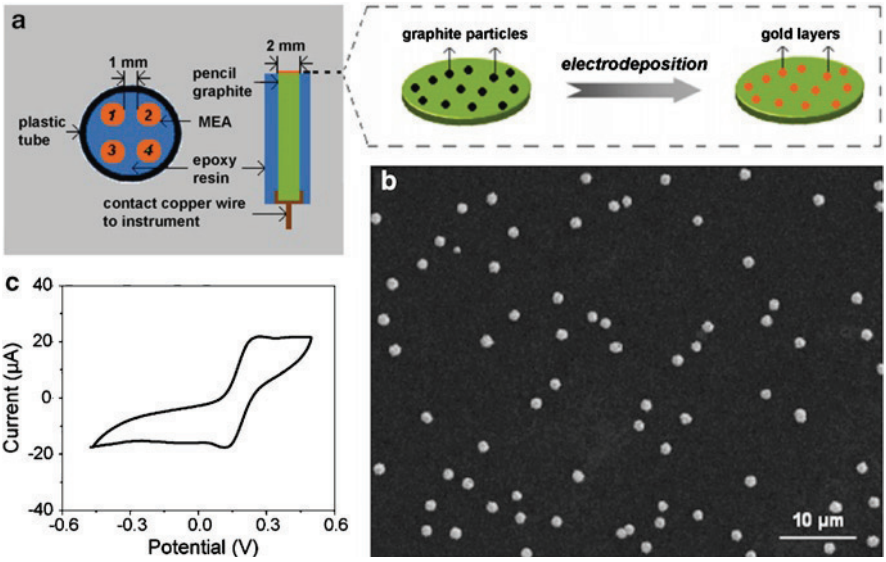

Fig. 2.23 (**a**) Schematic conformation of four individually addressable MEA platforms (*left*) with graphite particles coated with gold layers by electrodeposition (*right*); (**b**) a typical SEM image of the MEA platform after gold modification; (**c**) CV characterization of the above MEA platform measured in the presence of 10 mM $[Fe(CN)_6]^{3-/4-}$ with a scan rate of 0.1 V/s. Reprinted with permission from Zhang et al. [87]. © 2009, Elsevier

particles coated with gold layers as microelectrodes [87]. As shown in Fig. 2.23, the graphite particles available on the common pencil are utilized to direct the electrodeposition of gold layers with uniform microstructures, which displays a well-defined sigmoidal voltammetric response. In the concept-of-proof experiments, the resulting MEA platform is modified with a functionalized monolayer, on which antihuman IgG antibodies can be stably immobilized in a site-selective way through binding chemistry to selectively capture human IgG antigens from the sample media. The subsequent introduction of antihuman IgG antibodies (conjugated with 15-nm electroactive gold NPs), which recognize the captured IgG proteins, results in a significant decrease in the interfacial electron-transfer resistance. As shown in Fig. 2.24, a highly sensitive electrochemical quantification can be obtained through gold NP–amplified impedance responses. Thus, the MEA sensor can detect human IgG with a wider linear range (0.05–100 ng/mL) and a sensitivity over 10^3 larger than that of the conventional, bulk gold electrode.

2.3.4 Nanoparticle-Enhanced Voltammetric Signal

The Au NP-based amplification of voltammetric signals has also been characterized [88–90]. Li and Hu [91] developed an electrochemical determination method for

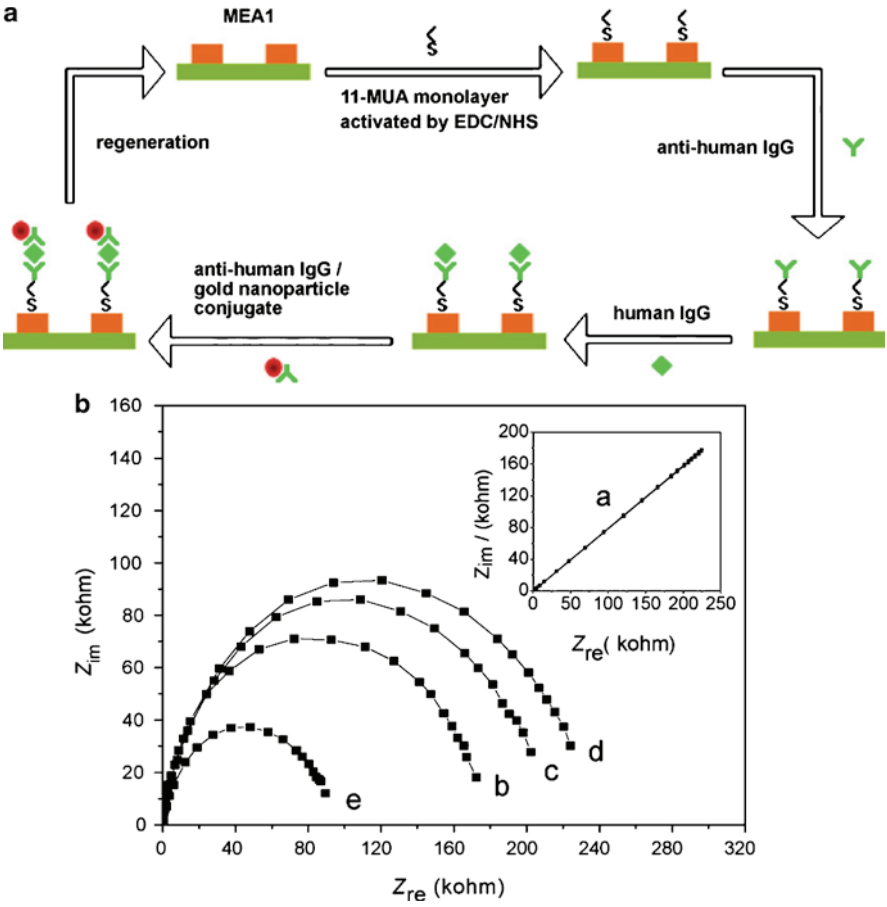

Fig. 2.24 (**a**) Schematic representation of successive fabrication, human IgG detection (5 ng/mL), and regeneration of an MEA platform-based immunosensor. (**b**) The corresponding Nyquist plots (Zim vs. Zre) for Faradaic impedance spectra in the presence of 10 mM $[Fe(CN)_6]^{3-/4-}$ at the MEA platform after (*a*) electrodeposition of the gold layer, (*b*) assembly of the 11-MUA monolayer, (*c*) covalent immobilization of antihuman IgG antibody, (*d*) binding of human IgG antigen, and (*e*) regeneration treatment. Reprinted with permission from Zhang et al. [87]. © 2009, Elsevier

analyzing sequence-specific DNA using ferrocene-capped gold NP–streptavidin conjugates. Thiolated DNA probes were covalently immobilized on a gold electrode, with hexanethiol forming a mixed self-assembled monolayer. After hybridization with tDNA, duplex DNA was formed on the gold surface. Then functional gold NPs were introduced via the strong interaction effect between biotin and streptavidin. The electrochemical signal of the ferrocene covering on the gold NPs was obviously enhanced in cyclic voltammetric and differential pulse voltammetric detection.

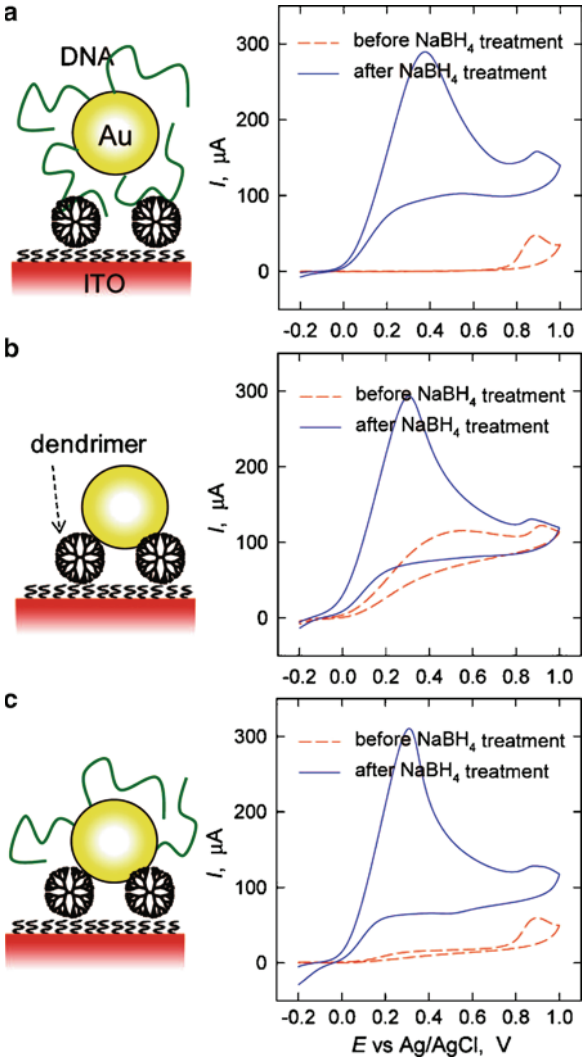

Fig. 2.25 Cyclic voltammograms obtained at (**a**) an ITO electrode modified with detection probe (DP)-conjugated Au NPs, (**b**) an Au NP-modified ITO electrode, and (**c**) an ITO electrode sequentially modified with Au NPs and DPs, in a 0.1 M phosphate buffer solution (pH 8) containing 2 mM hydrazine (at a scan rate of 50 mV/s) before and after $NaBH_4$ treatment for 15 min in Tris buffer (pH 9) containing 10 mM $NaBH_4$. Reprinted with permission from Das and Yang [92]. © 2009, American Chemical Society

Hydrazine can be electroxidated on bare Au NPs, while the electrooxidation is not observed on DNA-conjugated Au NPs (Fig. 2.25) [92]. Thus, when DNA-conjugated Au NPs are used as electrocatalytic labels in electrochemical DNA detection, the anodic current of hydrazine cannot be observed within the potential window because of the high overpotential caused by the slow electron-transfer kinetics on DNA-conjugated Au NPs as well as the slow electron tunneling between the Au NP and the ITO electrode. As $NaBH_4$ treatment can significantly enhance the electrocatalytic activity of DNA-conjugated AuNPs, it substantially decreases the overpotential caused by the slow electron-transfer kinetics; hence, the anodic current of hydrazine can be measured within the potential window if the distance between the Au NP and the ITO electrode is not too large. The enhancement with

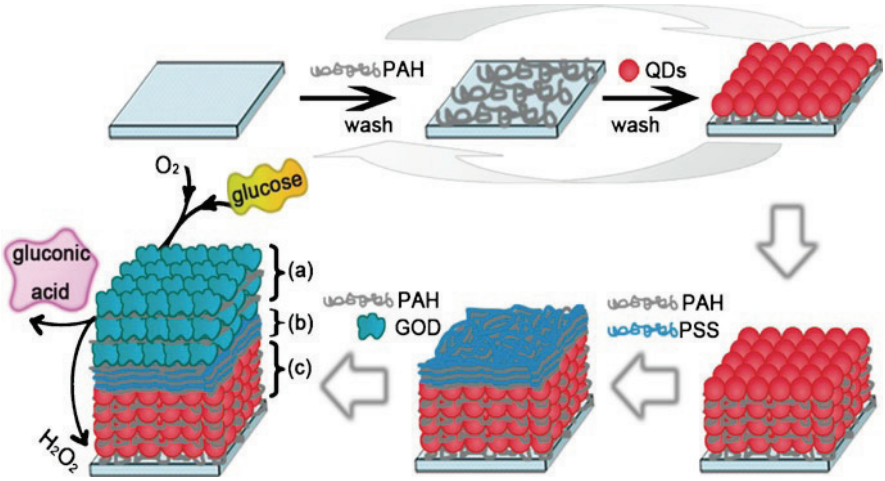

Fig. 2.26 Sensing assembly: (*a*) top three bilayers of PAH/GOD; (*b*) three bilayers of PAH/PSS; and (*c*) 12 bilayers of PAH/CdTe QDs. Reprinted with permission from Li et al. [93]. © 2009, American Chemical Society

$NaBH_4$ treatment produces a high signal current, and the low intrinsic electrocatalytic activity of ITO electrodes results in a low background current. This high signal-to-background ratio enables a detection limit of 1 fM DNA without target amplification or enzymatic signal amplification.

Li and coworkers [93] developed a blood glucose sensor based on the multilayer films of CdTe QDs and glucose oxidase (GOD) by using a layer-by-layer assembly technique (Fig. 2.26). When the composite films were contacted with glucose solution, the photoluminescence of QDs in the films was quickly quenched because the enzyme-catalyzed reaction product (H_2O_2) of GOD and glucose gave rise to the formation of surface defects on QDs. The quenching rate was a function of the concentration of glucose. The linear range and sensitivity for glucose determination could be adjusted by controlling the layers of QDs and GOD (Fig. 2.27). The biosensor could determine the concentration of blood glucose in real serum samples without sample pretreatment and exhibited satisfactory reproducibility and accuracy.

2.4 Nanoparticles as Carrier for Signal Amplification

2.4.1 Gold Nanoparticles as Tracer

Au NPs can also be used as carriers of the signaling molecules for amplification detection of DNA [94] and protein targets [95–97]. For example, Au NPs have been used as carriers of the signaling antibody anti-CA 15-3-HRP in order to achieve an amplification analysis of CA 15-3 antigen (Fig. 2.28) [97]. In the range

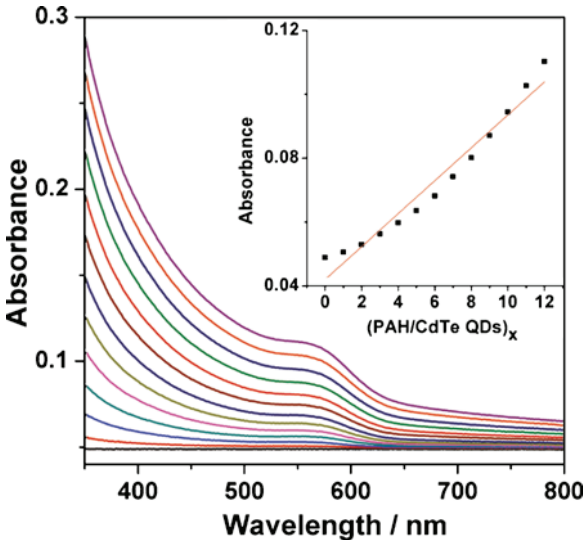

Fig. 2.27 UV-vis spectra of growing PAH/CdTe QD multilayers (1–12). *Inset* shows a plot of $\lambda = 567$ nm vs. the number of bilayers. Reprinted with permission from Li et al. [93]. © 2009, American Chemical Society

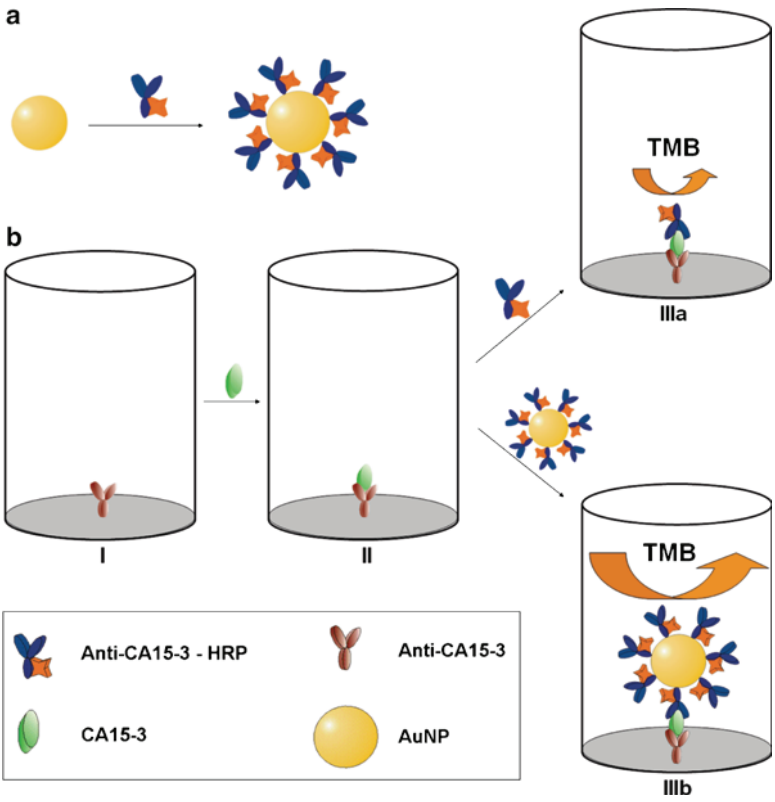

Fig. 2.28 Schematic (not to scale) of (**a**) the preparation of the Au–anti-CA15–3-HRP complex and (**b**) the sandwich-type ELISA procedure without (IIIa) and with (IIIb) the application of AuNPs as the signal enhancer. Reprinted with permission from Ambrosi et al. [97]. © 2010, American Chemical Society

between 0 and 60 U/mL, the assay adopting Au NPs as an enhancer results in higher sensitivity and shorter assay time when compared to classical ELISA procedures. Used an enzyme-labeled Au NP probe, Liu et al. developed a highly sensitive protein detection method [98]. As shown in Fig. 2.29, the enzyme-labeled Au NP probe is prepared by coating Au NP with antibody, single-stranded DNA (ssDNA), and HRP. Magnetic microparticle (MMP) functionalized with another antibody is used as the capture probe. The target protein is sandwiched by the enzyme-labeled Au NP probe and the capture probe through immunoreaction, and the target immunoreaction event can be sensitively transduced via the enzymatically amplified optical signal. The detection limit of CEA for this strategy is 12 ng/L, which is approximately 130 times more sensitive than the conventional ELISA.

Using a nanoporous gold (NPG) electrode and HRP-labeled secondary antibody–Au NP bioconjugates, a highly sensitive protein detection method has been described (Fig. 2.30) [99]. The electroactive product of ophenylenediamine (OPD) oxidized with H_2O_2 catalyzed by HRP is reduced in the Britton–Robinson buffer, the peak current of which is used to determine the concentration of antigen in the sample. The active surface area of the NPG electrode is larger than that of a bare flat one, and the presence of Au NPs enhances the immobilized amount of HRP-labeled antibody. The sensitivity of the immunoassay for the determination of the target protein is increased significantly. A detection range of 0.01–1.0 ng/mL is obtained for hepatitis B surface antigen (HBs-Ag), and the detection limit is 2.3 pg/mL, which is about 100 times more sensitive than ELISA.

Figure 2.31 shows a sensitive CLIA based on MBs and HRP-labeled anti-AFP-modified Au NPs for the determination of AFP antigen [100]. A new CL enhancer, bromophenol blue (BPB), is employed in the CLIA. Due to the magnetic separation and amplification feature of Au NPs as HRP labels, the CLIA offers a linear detection range from 0.1 to 5.0 ng/mL ($R = 0.9997$) and a detection limit of 0.01 ng/mL (3σ) for AFP. This detection limit is one order of magnitude lower than that obtained without using Au NPs, and much lower than that typically achieved by ELISA.

Using Au NPs to immobilize capture aptamers, Fang et al. [101] proposed an electrochemiluminescence aptasensor for the sensitive and cost-effective detection of the target thrombin. As shown in Fig. 2.32, capture aptamers labeled with Au NPs were first immobilized onto the thio-silanized ITO electrode surface. After catching the target thrombin, signal aptamers tagged with ECL labels were attached to the assembled electrode surface, forming an Au NP-capture–aptamer/thrombin/ECL-tagged signal–aptamer sandwich type. Treating the resulting electrode surface with tri-*n*-propylamine (TPA) and applying a swept potential to the electrode, an ECL response was generated that detected the target protein. The signal-to-dose curve followed a sandwich format equation, and a detection limit of 10-nM thrombin could be estimated by this strategy.

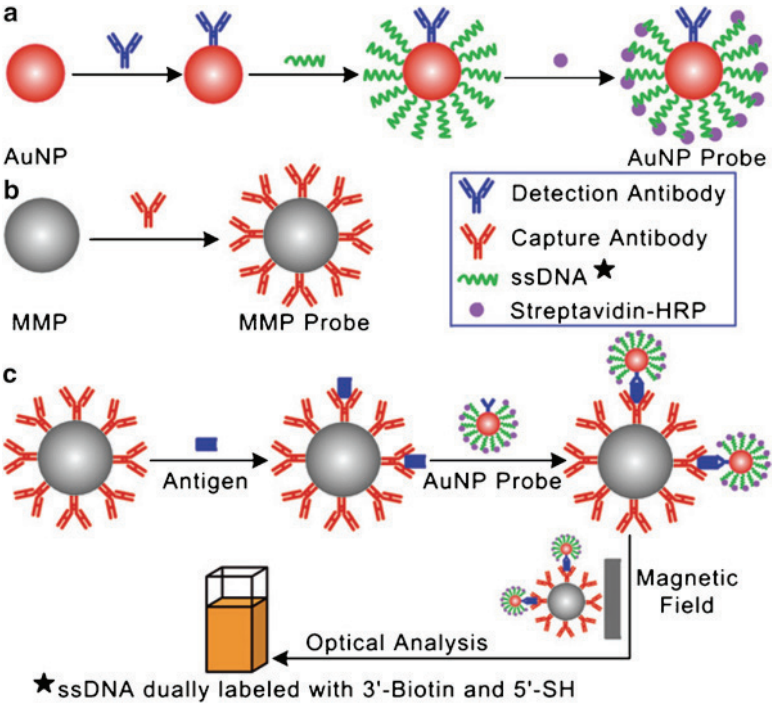

Fig. 2.29 Schematic diagrams of the preparation of the (**a**) enzyme-labeled Au NP probes and (**b**) MMP probes. (**c**) Schematic illustration of the enzyme-labeled Au NP probe-based immunoassay processes. Reprinted with permission from Liu et al. [98]. © 2010, Royal Society of Chemistry

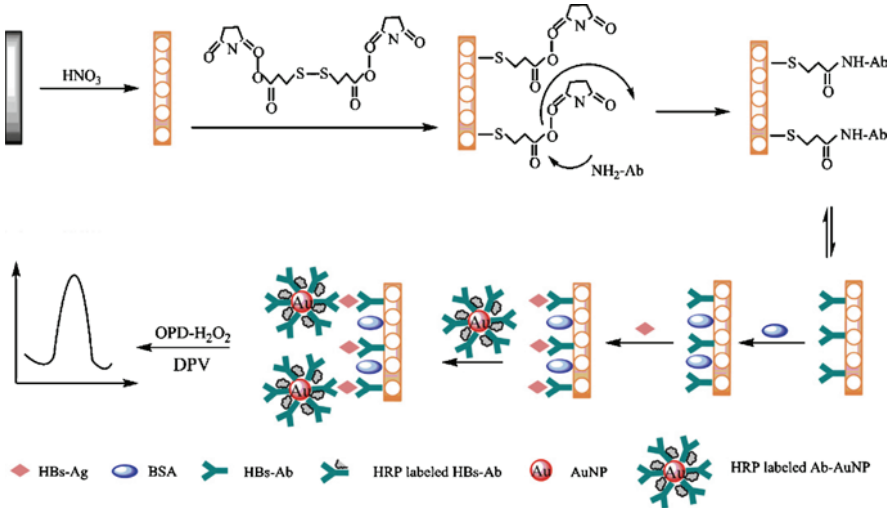

Fig. 2.30 Schematic illustration of the stepwise process of the modified electrode. Reprinted with permission from Ding et al. [99]. © 2010, Elsevier

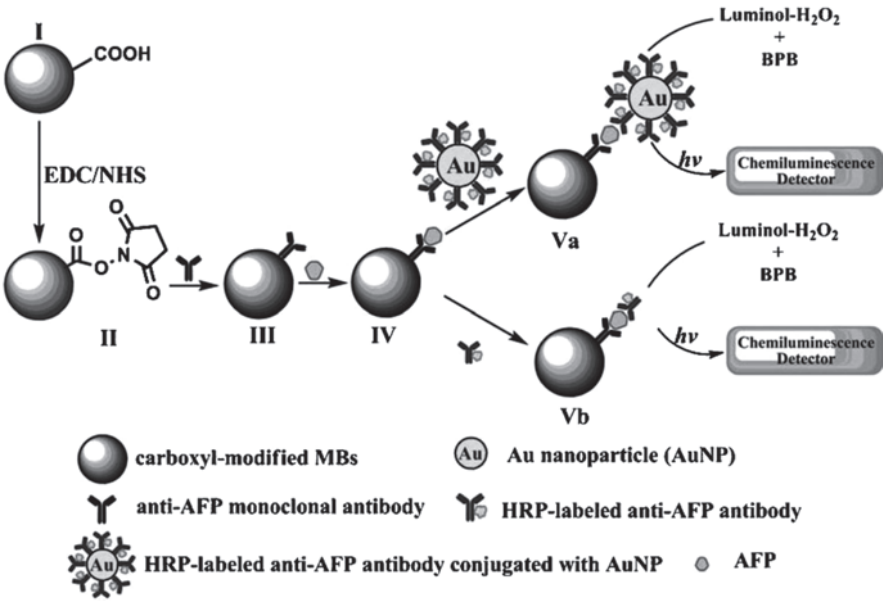

Fig. 2.31 The schematic illustration of the determination of AFP based on the sandwich-type chemiluminescence immunoassay. Reprinted with permission from Bi et al. [100]. © 2009, Wiley

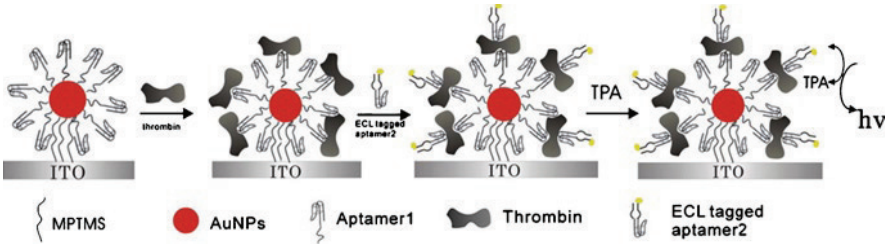

Fig. 2.32 The schematic diagram of the fabrication of the ECL aptasensor. Reprinted with permission from Fang et al. [101]. © 2008, Elsevier

Using Au NP-based signal amplification, an electrochemical sensor has been designed for the highly sensitive detection of Hg^{2+} ions in aqueous solution [102]. A T-rich mercury-specific oligonucleotide probe (MSO) (5′-TTCTTTCTTCCCCTT GTTTGTT-3′) is used to selectively bind with Hg^{2+}. In the presence of Hg^{2+}, the complex of Hg^{2+} with thymines yields a stable hairpin structure [103]. Normally, the MSO probe is directly immobilized on Au electrode surfaces to capture Hg^{2+} in aqueous solution (Fig. 2.33a), and the electrochemical reduction of surface-confined Hg^{2+} provides a readout signal for the quantitative detection of Hg^{2+}. However, the sensitivity of this Hg^{2+} sensor can be improved by more than three orders of magnitude with Au NP-based signal amplification, in which Au NPs are comodified

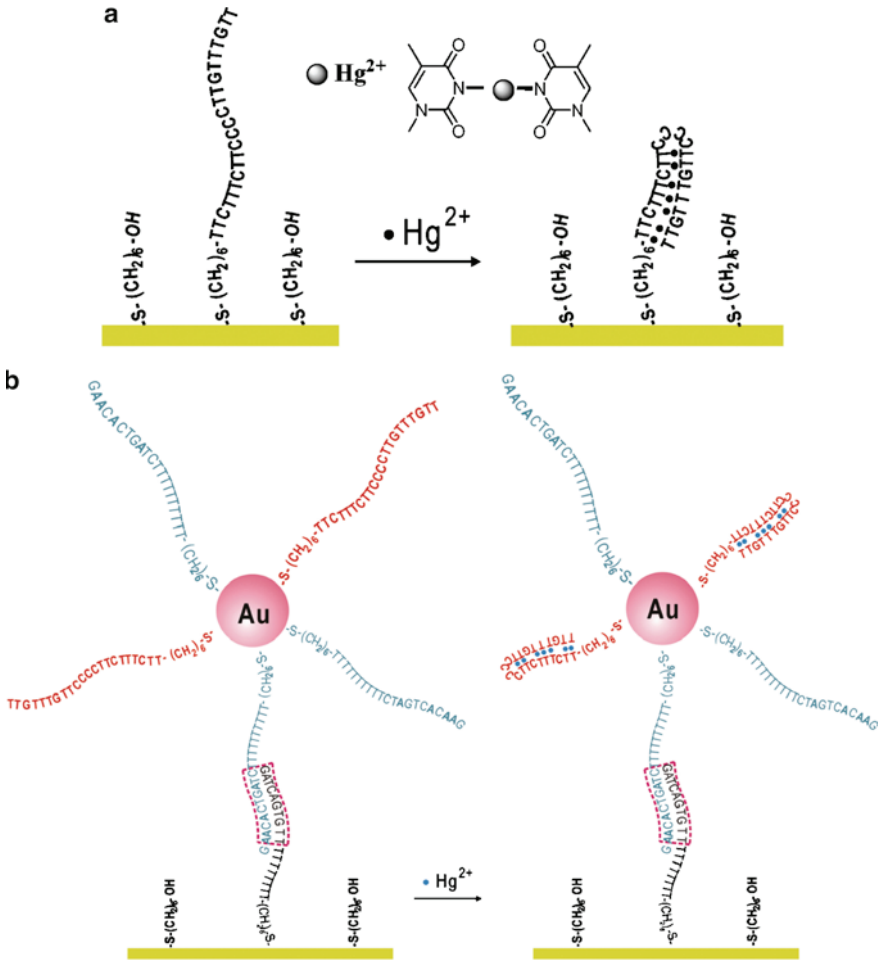

Fig. 2.33 (**a**) Directly immobilized MSO probe and (**b**) Au NP-mediated immobilized MSO probe. Reprinted with permission from Zhu et al. [102]. © 2009, American Chemical Society

with the MSO probe and a linking probe that is complementary to a cDNA probe immobilized on gold electrodes (Fig. 2.33b).

Using Au NPs to load many CdS NP-labeled linker DNA, a significant amplification for the detection of thrombin has been obtained [104]. As shown in Fig. 2.34, aptamers are immobilized on the Au NP-modified electrode to construct the sandwich-type detection strategy. The concentration of thrombin is monitored based upon the concentration of dissolved Cd^{2+} formed in the dissolution of CdS by acid treatment and quantified by differential pulse voltammetry. Thrombin can be detected in the linear range of 1.0×10^{-15}–1.0×10^{-11} M, with a detection limit of 5.5×10^{-16} M. A similar strategy has been conducted by Zhang's group based on bio-barcode techniques [105].

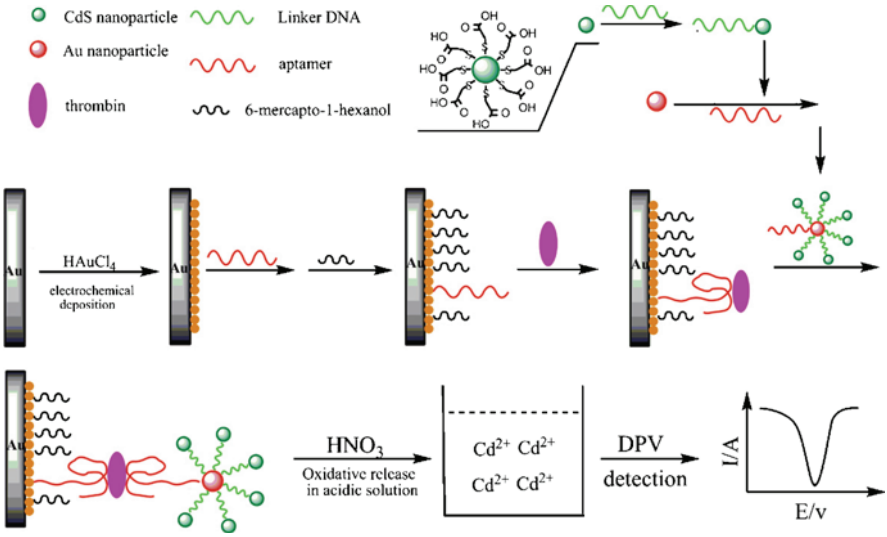

Fig. 2.34 The scheme of the electrochemical determination of thrombin based on aptamer. Reprinted with permission from Ding et al. [105]. © 2010, Elsevier

Taking the advantage of the catalytic reaction of DNAzyme upon its binding to Pb^{2+} and the use of DNA–Au bio-barcodes to achieve signal enhancement, an electrochemical DNAzyme sensor for the sensitive and selective detection of Pb^{2+} has been developed [106]. As shown in Fig. 2.35, a specific DNAzyme for Pb^{2+} is immobilized onto the Au electrode surface via a thiol–Au interaction. The DNAzyme hybridizes to a specially designed complementary substrate strand that has an overhang, which in turn hybridizes to the DNA–Au bio-barcode. A redox mediator, $Ru(NH_3)_6^{3+}$, which can bind to the anionic phosphate of DNA through electrostatic interactions, serves as the electrochemical signal transducer. Upon binding of Pb^{2+} to the DNAzyme, the DNAzyme catalyzes the hydrolytic cleavage of the substrate, resulting in the removal of the substrate strand along with the DNA–Au bio-barcode and the bound $Ru(NH_3)_6^{3+}$ from the Au electrode's surface. The release of $Ru(NH_3)_6^{3+}$ results in a lower electrochemical signal of $Ru(NH_3)_6^{3+}$ confined on the electrode's surface. The differential pulse voltammetric signals of $Ru(NH_3)_6^{3+}$ provide quantitative measurements of the Pb^{2+} concentrations, with a linear calibration range from 5 nM to 0.1 μM. Because each NP carries a large number of DNA strands that bind to the signal transducer molecule $Ru(NH_3)_6^{3+}$, the use of DNA–Au bio-barcodes enhances the detection sensitivity, enabling the detection of Pb^{2+} at a very low level (1 nM).

A densely packed gold NP platform combined with a multiple-enzyme-labeled detection antibody–MB bioconjugate has been used as the basis for preparing an ultrasensitive electrochemical immunosensor to detect cancer biomarkers in serum [107]. As shown in Fig. 2.36, the sensor is fabricated by alternate layer-by-layer electrostatic adsorption of a dense glutathione-decorated Au NP and an underlying layer of cationic poly(diallyldimethyl ammonium chloride) on a pyrolytic graphite

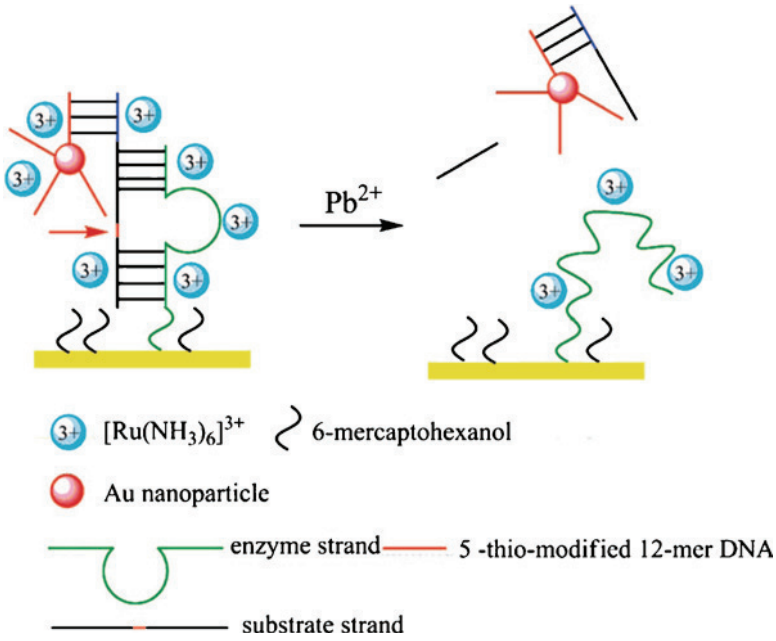

Fig. 2.35 The principle of the electrochemical DNAzyme sensor for Pb^{2+}. Reprinted with permission from Shen et al. [106]. © 2008, American Chemical Society

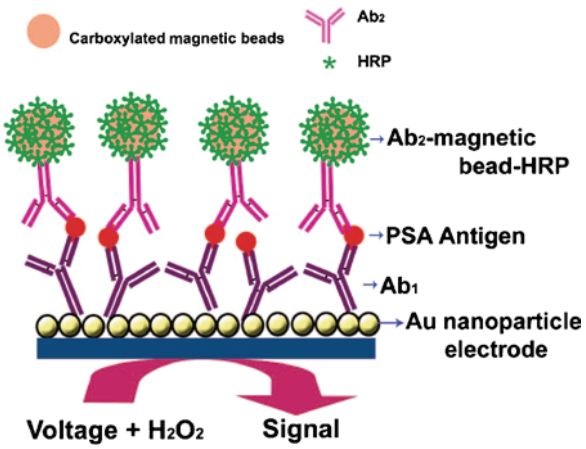

Fig. 2.36 Au NP immunosensor with Ab_1 attached that has captured an antigen from a sample after treating with Ab_2–magnetic bead (MB)–HRP providing multiple enzyme labels for each PSA. The detection step involves immersing the immunosensor into buffer containing mediator, applying voltage, and injecting H_2O_2. Reprinted with permission from Mani et al. [107]. © 2009, American Chemical Society

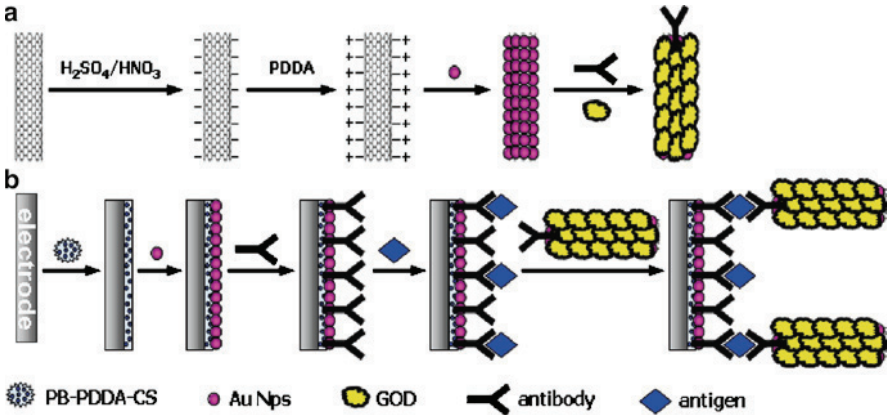

Fig. 2.37 Schematic representation of the (**a**) preparation procedure of GOD–Au NPs/CNTs–Ab_2 tracer and (**b**) preparation of immunosensors and sandwich-type electrochemical immunoassay. Reprinted with permission from Lai et al. [109]. © 2009, American Chemical Society

electrode. The capture antibody is attached to the Au NP-modified electrode to detect PSA in serum. Highly amplified detection is achieved by using multilabeled bioconjugates made by linked multiple HRP and detection antibodies to carboxylated MBs for signal development. This represents an ultralow mass detection limit of 5 fg of PSA.

2.4.2 Carbon Nanotubes as Carrier

CNTs are a good carrier for biomolecules and signal molecules [108, 109]. As shown in Fig. 2.37, the immunosensor array is constructed by coating layer by layer colloidal Prussian blue (PB), gold NPs, and capture antibodies on screen-printed carbon electrodes. The preparation of GOD-functionalized nanocomposites and the labeling of antibody are performed by the one-pot assembly of GOD and antibody on gold NP-attached CNTs (Fig. 2.37b). The PB immobilized on the immunosensor's surface acts as a mediator to catalyze the reduction of H_2O_2 produced in the enzymatic cycle. Both the high-content GOD and CNTs in the tracer amplify the detectable signal for the sandwich-type immunoassay. The simultaneous multiplexed immunoassay method can offer linear ranges of three orders of magnitude, with the detection limits down to 1.4 and 2.2 pg/mL for CEA and α-fetoprotein, respectively.

Using CNT-based labels, Lee et al. developed an amplified nucleic acid detection [110]. As shown in Fig. 2.38, the CNT-based labels were synthesized based on diimideactivated amidation. The DPs were prelabeled with HRP enzymes cross-linked by glutaraldehyde. The carboxylated SWNTs were covalently functionalized with prelabeled DPs by reacting with the amine group at the 5′-end of DPs with carboxylic acid

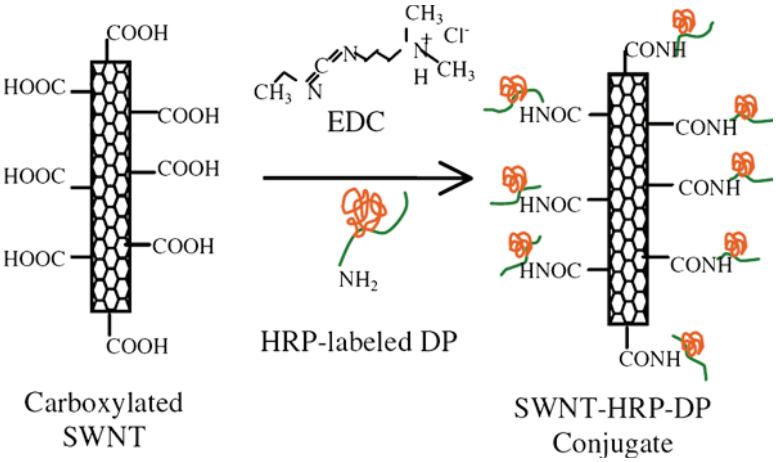

Fig. 2.38 Diimide-activated amidation for conjugation of SWNT–HRP–DP. Reprinted with permission from Lee et al. [110]. © 2007, IOP Publishing Ltd.

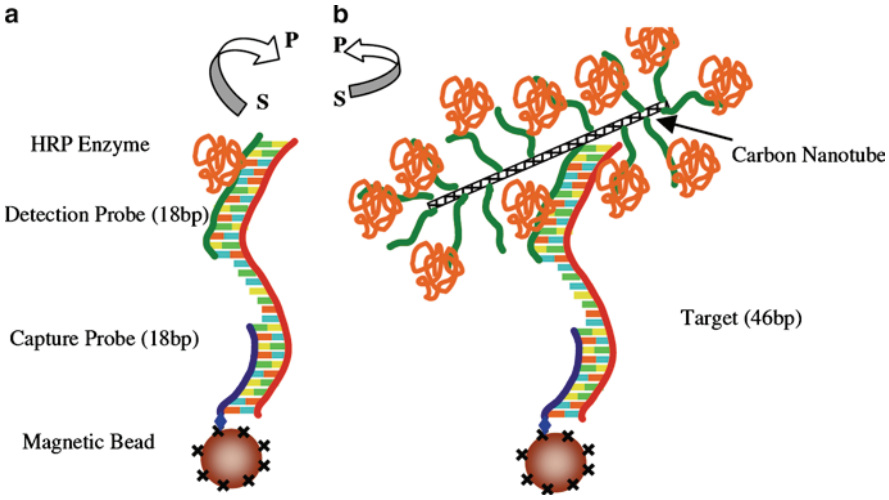

Fig. 2.39 Schematic representation of the signal amplification for sandwich hybridization assay performed on MBs. The signal-to-single hybridization event ratio of (**a**) the conventional HRP label is amplified by (**b**) multiple HRP and DP-conjugated CNT-based labels. Reprinted with permission from Lee et al. [110]. © 2007, IOP Publishing Ltd.

groups on SWNTs in the presence of the cross-linker *N*-(3-dimethylaminopropyl)-*N′*-ethylcarbodiimide hydrochloride. The resulting CNT labels significantly enhanced the nucleic acid assay sensitivity by at least 1,000 times compared to that of conventional labels used in enzyme-linked oligosorbent assay (Fig. 2.39), enabling the detection of a four-order-wide dynamic range of target concentrations, with a detection limit of 1×10^{-12} M (60×10^{-18} mol in 60 μL).

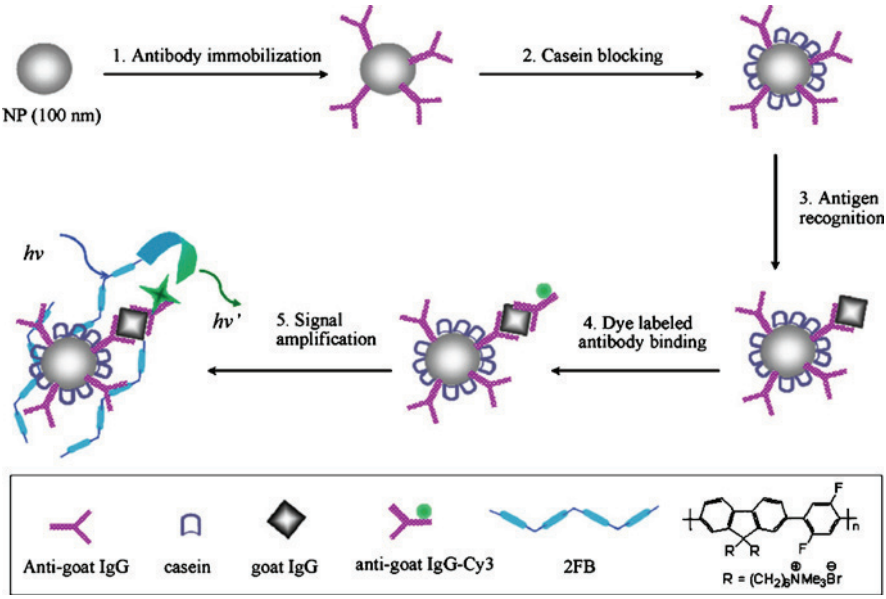

Fig. 2.40 Schematic illustration of the CCP-amplified NP-based fluoroimmunoassay. Reprinted with permission from Wang and Liu [111]. © 2009, Elsevier

2.4.3 Silica Nanoparticles as Carrier

Due to the small size, high surface-to-volume ratio, and good biocompatibility, silica NPs have become another normally used carrier for biomolecule immobilization. For example, based on silica NPs, Wang and Liu [111] developed a fluoroimmunoassay for antigen detection and quantification. As shown in Fig. 2.40, after immobilization of the prime antibody on the silica NP surface, the NPs were used to capture antigen and Cy3-labeled secondary antibody in a sandwich assay format. The presence of target antigen in solution brought the fluorescent Cy3 molecules to the NP's surface. The addition of a cationic conjugated polymer (CCP) further amplified the fluorescence signal of the dye and improved the assay sensitivity. Due to the pink color of the Cy3 molecules, the assay allowed a detection limit of 50 ng/mL of IgG by naked-eye detection.

Mesoporous silica nanoparticles (MSN) have also been used as molecule carrier to improve detection sensitivity. For example, Yang et al. [112] designed an MSN-based label by loading MSN with mediator thionine (TH), enzyme HRP, and secondary antihuman IgG antibody for IgG detection (Fig. 2.41). The sensitivity of the sandwich-type immunosensor could greatly improved, leading to a detection range of 0.01–10 ng/mL of human IgG.

The electrochemiluminescence of doped silica nanoparticles (DSNPs), prepared by a reverse microemulsion method that leads to the covalent incorporation of the $Ru(bpy)_3^{2+}$, has been investigated in acetonitrile and aqueous buffers [113].

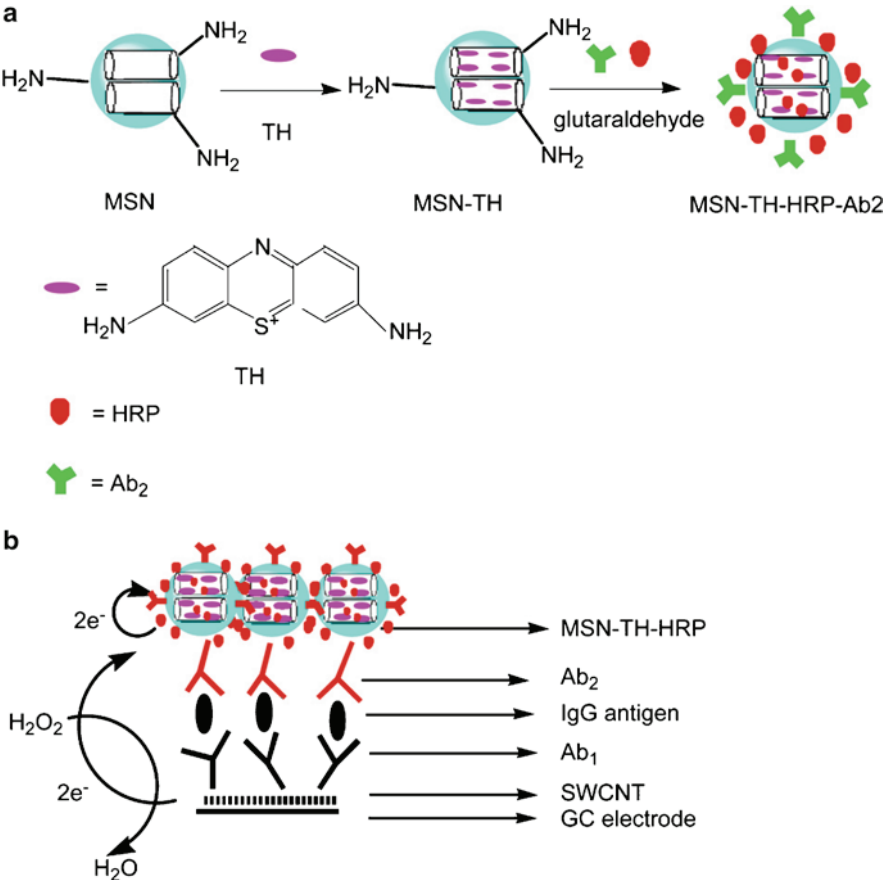

Fig. 2.41 Schematic representation of the preparation of the (**a**) MSN–TH–HRP–Ab_2 and (**b**) immunosensor. Reprinted with permission from Yang et al. [112]. © 2010, Elsevier

The ECL intensity obtained by such functionalized substrates in aqueous media, using tripropylamine (TPrA) as coreactant, is surprisingly increased with respect to direct electrochemical oxidation because of the ability of oxidized TPrA to diffuse within the DSNP's structure and reach a higher number of emitting units with respect to direct electron tunneling. A more than 1,000-fold increase in the ECL signal can be received by the chemically and electrochemically stable DSNP compared to that of a single dye, suggesting that this nanostructure as luminescent labels represents a very promising system for ultrasensitive bioanalysis.

Using CdTe QD-functionalized silica nanosphere labels, Chen et al. [114] designed an electrochemical immunsensor for protein detection. As shown in Fig. 2.42, AFP antibody was covalently binded to CdTe QDs on the surface of silica NPs. Enhanced sensitivity can be achieved based on an increase in CdTe QDs loading per sandwiched immunoreaction (Fig. 2.43).

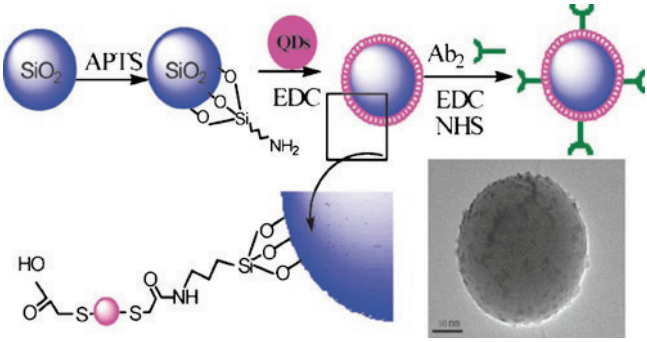

Fig. 2.42 Preparation process of Si/QD/Ab_2. *Inset*: TEM image of the resultant Si/QD/Ab_2. Reprinted with permission from Chen et al. [114]. © 2009, Royal Society of Chemistry

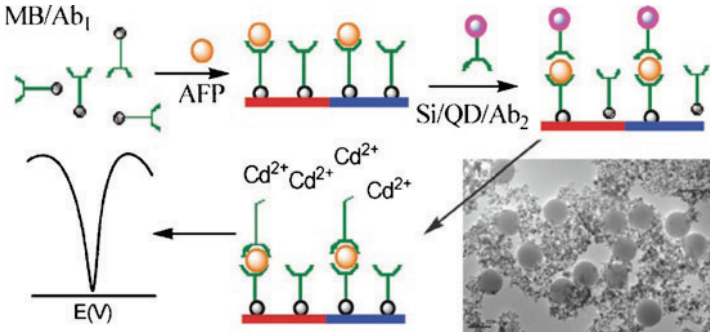

Fig. 2.43 Sandwiched immunoassay process using Si/QD/Ab_2 as labels. *Inset*: TEM image of MB/Ab_1–Ag–Si/QD/Ab_2. Reprinted with permission from Chen et al. [114]. © 2009, Royal Society of Chemistry

2.4.4 Other Materials as Carrier

A NP label capable of amplifying the electrochemical signal of DNA hybridization has been fabricated by functionalizing poly(styrene-co-acrylic acid) microbeads with CdTe QDs [115]. As shown in Fig. 2.44, CdTe-tagged polybeads are prepared by a layer-by-layer self-assembly of the CdTe QDs and polyelectrolyte on the polybeads. The CdTe-tagged polybeads are then attached to DNA probes specific to breast cancer by streptavidin–biotin binding to construct a DNA biosensor. The detection of the DNA hybridization process is achieved by the square-wave voltammetry of Cd^{2+} after the dissolution of the CdTe tags with HNO_3. The efficient carrier-bead amplification platform, coupled with the highly sensitive stripping voltammetric measurement, gives rise to a detection limit of 0.52 fmol/L and a dynamic range spanning five orders of magnitude.

Figure 2.45 shows a novel NP-based electrochemical immunoassay of CA125 coupling with a microfluidic strategy [116]. To construct the immunoassay,

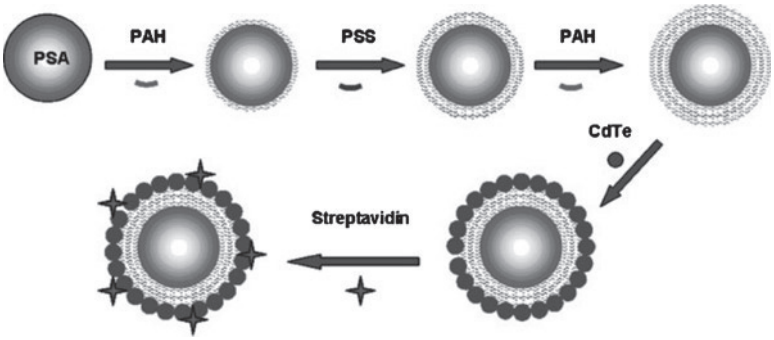

Fig. 2.44 Schematic diagram of the assembly process for the preparation of streptavidin/CdTe-tagged polybeads. Reprinted with permission from Dong et al. [115]. © 2010, Wiley

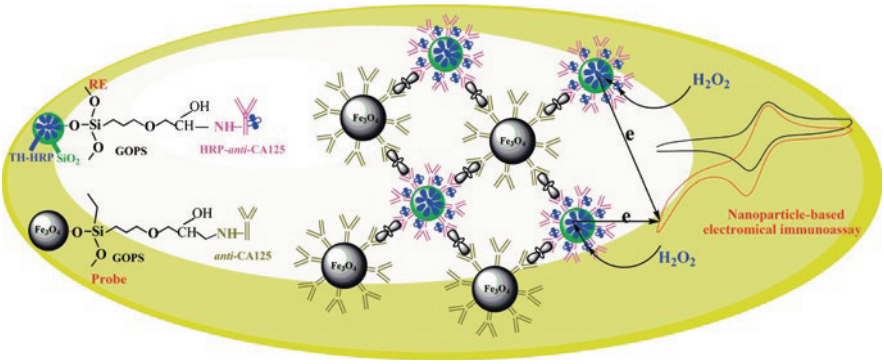

Fig. 2.45 Construction of the immunosensing probe and recognition element and measurement protocol of the NP-based electrochemical immunoassay with a sandwich-type format. Reprinted with permission from Tang et al. [116]. © 2010, American Chemical Society

thionine–horseradish peroxidase conjugation (TH-HRP) is initially doped into nanosilica particles using the reverse-micelle method, and then HRP-labeled anti-CA125 antibodies (HRP-anti-CA125) are bound onto the surface of the synthesized NPs. The sandwich-type immunoassay format is used for the online formation of the immunocomplex in an incubation cell and captured in the detection cell with an external magnet. The electrochemical signal is derived from the carried HRP toward the reduction of H_2O_2 using the doped TH as electron mediator. A wide working range of 0.1–450 U/mL, with a detection limit of 0.1 U/mL CA125, can be obtained. The assay has been evaluated for clinical serum samples and has yielded results that are in excellent accordance with the results obtained from the standard ELISA method.

2.5 Conclusions

Nanotechnology offers unique opportunities for designing ultrasensitive bioassays. The studies demonstrate the broad potential of bioconjugated NPs for the amplified transduction of biomolecular recognition events. Given the enormous amplification afforded by NP tracers, such nanomaterials provide the basis for ultrasensitive assays of proteins and nucleic acids. The remarkable sensitivity of the new nanomaterial-based sensing protocols opens up the possibility of detecting disease markers, biothreat agents, or infectious agents that cannot be measured by conventional methods. Due to the diverse properties of different nanomaterials, utilizing two or more types of nanomaterials can enhance the good qualities as well as offset the insufficiency of each individual nanomaterial, which can produce better results than those obtained using only one type of nanomaterial. The use of NP tags to detect proteins is still in its infancy, but the lessons learned in ultrasensitive DNA detection should provide useful starting points. The successful realization of the new signal-amplification strategies requires proper attention to nonspecific adsorption issues that commonly control the detectability of bioaffinity assays. Proper washing and surface blocking steps should thus be employed to avoid the amplification of background signals (associated with nonspecific adsorption of the nanoparticle amplifiers). A wide range of newly introduced nanomaterials is expected to further expand the realm of nanomaterial-based biosensors.

References

1. Mulvaney, P.: Surface plasmon spectroscopy of nanosized metal particles. Langmuir **12**, 788–800 (1996)
2. Alvarez, M.M., Khoury, J.T., Schaaff, T.G., et al.: Optical absorption spectra of nanocrystal gold molecules. J. Phys. Chem. B **101**, 3706–3712 (1997)
3. Alivisatos, A.P.: Perspectives on the physical chemistry of semiconductor nanocrystals. J. Phys. Chem. **100**, 13226–13239 (1996)
4. Brus, L.E.: Quantum crystallites and nonlinear optics. Appl. Phys. A Mater. **53**, 465–474 (1991)
5. Shipway, A.N., Katz, E., Willner, I.: Nanoparticle arrays on surfaces for electronic, optical, and sensor applications. ChemPhysChem. **1**, 18–52 (2000)
6. Khairutdinov, R.F.: Physical chemistry of nanocrystalline semiconductors. Colloid J. **59**, 535–548 (1997)
7. Lewis, L.N.: Chemical catalysis by colloids and clusters. Chem. Rev. **93**, 2693–2730 (1993)
8. Kesavan, V., Sivanand, P.S., Chandrasekaran, S., et al.: Catalytic aerobic oxidation of cycloalkanes with nanostructured amorphous metals and alloys. Angew. Chem. Int. Ed. **38**, 3521–3523 (1999)
9. Ahuja, R., Caruso, P.L., Mbius, D., et al.: Formation of molecular strands by hydrogen bonds at the gas-water interface: molecular recognition and quantitative hydrolysis of barbituric acid lipids. Angew. Chem. Int. Ed. **32**, 1033–1036 (1993)
10. He, L., Musick, M.D., Nicewarner, S.R., et al.: Colloidal Au-enhanced surface plasmon resonance for ultrasensitive detection of DNA hybridization. J. Am. Chem. Soc. **122**, 9071–9077 (2000)
11. Kubitschko, S., Spinke, J., Bruckner, T., et al.: Sensitivity enhancement of optical immunosensors with nanoparticles. Anal. Biochem. **253**, 112–122 (1997)
12. Lyon, L.A., Musick, M.D., Natan, M.J.: Colloidal Au-enhanced surface plasmon resonance immunosensing. Anal. Chem. **70**, 5177–5183 (1998)

13. Englebienne, P., Hoonacker, A.V., Verhas, M.: High-throughput screening using the surface plasmon resonance effect of colloidal gold nanoparticles. Analyst **126**, 1645–1651 (2001)
14. Niemeyer, C.M.: Nanoparticles, proteins, and nucleic acids: biotechnology meets materials science. Angew. Chem. Int. Ed. **40**, 4128–4158 (2001)
15. Palmer, R.E., Guo, Q.: Imaging thin films of organic molecules with the scanning tunnelling microscope. Phys. Chem. Chem. Phys. **4**, 4275–4284 (2002)
16. Chen, Z., He, Y.J., Luo, S.L., et al.: Label-free colorimetric assay for biological thiols based on ssDNA/silver nanoparticle system by salt amplification. Analyst **135**, 1066–1069 (2010)
17. Riboh, J.C., Haes, A.J., McFarland, A.D., et al.: Nanoscale optical biosensor: real-time immunoassay in physiological buffer enabled by improved nanoparticle adhesion. J. Phys. Chem. B **107**, 1772–1780 (2003)
18. Moon, S., Kim, D.J., Kim, K., et al.: Surface-enhanced plasmon resonance detection of nanoparticle-conjugated DNA hybridization. Appl. Opt. **49**, 484–491 (2010)
19. Maier, I., Morgan, M.R.A., Lindner, W., et al.: Optical resonance-enhanced absorption-based near-field immunochip biosensor for allergen detection. Anal. Chem. **80**, 2694–2703 (2008)
20. Xu, S.P., Ji, X.H., Xu, W.Q., et al.: Immunoassay using probe-labelling immunogold nanoparticles with silver staining enhancement via surface-enhanced Raman scattering. Analyst **129**, 63–68 (2004)
21. Grubisha, D.S., Lipert, R.J., Park, H.Y., et al.: Femtomolar detection of prostate-specific antigen: an immunoassay based on surface-enhanced Raman scattering and immunogold labels. Anal. Chem. **75**, 5936–5943 (2003)
22. Hsu, H.Y., Huang, Y.Y.: RCA combined nanoparticle-based optical detection technique for protein microarray: a novel approach. Biosens. Bioelectron. **20**, 123–126 (2004)
23. Joung, H.A., Lee, N.R., Lee, S.K., et al.: High sensitivity detection of 16s rRNA using peptide nucleic acid probes and a surface plasmon resonance biosensor. Anal. Chim. Acta **630**, 168–173 (2008)
24. Yao, X., Li, X., Toledo, F., et al.: Sub-attomole oligonucleotide and p53 cDNA determinations via a high-resolution surface plasmon resonance combined with oligonucleotide-capped gold nanoparticle signal amplification. Anal. Biochem. **354**, 220–228 (2006)
25. Law, W.C., Yong, K.T., Baev, A., et al.: Nanoparticle enhanced surface plasmon resonance biosensing: application of gold nanorods. Opt. Express **17**, 19041–19046 (2009)
26. Liu, X., Dai, Q., Austin, L., et al.: A one-step homogeneous immunoassay for cancer biomarker detection using gold nanoparticle probes coupled with dynamic light scattering. J. Am. Chem. Soc. **130**, 2780–2782 (2008)
27. Hsieh, B.Y., Chang, Y.F., Ng, M.Y., et al.: Localized surface plasmon coupled fluorescence fiber-optic biosensor with gold nanoparticles. Anal. Chem. **79**, 3487–3493 (2007)
28. Li, J.S., Deng, T., Chu, X., et al.: Rolling circle amplification combined with gold nanoparticle aggregates for highly sensitive identification of single-nucleotide polymorphisms. Anal. Chem. **82**, 2811–2816 (2010)
29. Li, J., Song, S.P., Li, D., et al.: Multi-functional crosslinked Au nanoaggregates for the amplified optical DNA detection. Biosens. Bioelectron. **24**, 3311–3315 (2009)
30. Zhang, J.Q., Wang, Y.S., He, Y., et al.: Determination of urinary adenosine using resonance light scattering of gold nanoparticles modified structure-switching aptamer. Anal. Biochem. **397**, 212–217 (2010)
31. Liu, X., Huo, Q.: A washing-free and amplification-free one-step homogeneous assay for protein detection using gold nanoparticle probes and dynamic light scattering. J. Immunol. Methods **349**, 38–44 (2009)
32. Kim, D., Daniel, W.L., Mirkin, C.A.: Microarray-based multiplexed scanometric immunoassay for protein cancer markers using gold nanoparticle probes. Anal. Chem. **81**, 9183–9187 (2009)
33. Reynolds, R.A., Mirkin, C.A., Letsinger, R.L., et al.: Nanoparticle-based quantitative colorimetric detection of oligonucleotides. J. Am. Chem. Soc. **122**, 3795–3796 (2000)
34. Xu, W., Xue, X.J., Li, T.H., et al.: Ultrasensitive and selective colorimetric DNA detection by nicking endonuclease assisted nanoparticle amplification. Angew. Chem. Int. Ed. **48**, 6849–6852 (2009)

35. Aslan, K., Gryczynski, I., Malicka, J., et al.: Metal-enhanced fluorescence: an emerging tool in biotechnology. Curr. Opin. Biotechnol. **16**, 55–62 (2005)
36. Lakowicz, J.R.: Plasmonics in biology and plasmon-controlled fluorescence. Plasmonics **1**, 5–33 (2006)
37. Stewart, M.E., Anderton, C.R., Thompson, L.B.: Nanostructured plasmonic sensors. Chem. Rev. **108**, 494–521 (2008)
38. Corrigan, T.D., Guo, S., Phaneuf, R.J., et al.: Enhanced fluorescence from periodic arrays of silver nanoparticles. J. Fluoresc. **15**, 777–784 (2005)
39. Sabanayagam, C.R., Lakowicz, J.R.: Increasing the sensitivity of DNA microarrays by metal-enhanced fluorescence using surface-bound silver nanoparticles. Nucleic Acids Res. **35**, e13 (2007)
40. Guo, S.H., Tsai, S.J., Kan, H.C., et al.: The effect of an active substrate on nanoparticle-enhanced fluorescence. Adv. Mater. **20**, 1424–1428 (2008)
41. Kulakovich, O., Strekal, N., Yaroshevich, A., et al.: Enhanced luminescence of CdSe quantum dots on gold colloids. Nano Lett. **2**, 1449–1452 (2002)
42. Bardhan, R., Grady, N.K., Cole, G.R., et al.: Fluorescence enhancement by Au nanostructures: nanoshells and nanorods. ACS Nano **3**, 744–752 (2009)
43. Hayakawa, T., Selvan, S.T., Nogami, M.: Field enhancement effect of small Ag particles on the fluorescence from Eu^{3+} -doped SiO_2 glass. Appl. Phys. Lett. **74**, 1513–1515 (1999)
44. Mackowski, S., Wormke, S., Maier, A.J., et al.: Metal-enhanced fluorescence of chlorophylls in single light-harvesting complexes. Nano Lett. **8**, 558–564 (2008)
45. Lakowicz, J.R.: Radiative decay engineering 5: metal-enhanced fluorescence and plasmon emission. Anal. Biochem. **337**, 171–194 (2005)
46. Fu, Y., Zhang, J., Lakowicz, J.R.: Silver-enhanced fluorescence emission of single quantum dot nanocomposites. Chem. Commun. **3**, 313–315 (2009)
47. Tovmachenko, O.G., Graf, C., Van Den Heuvel, D.J., et al.: Fluorescence enhancement by metal-core/silica-shell nanoparticles. Adv. Mater. **18**, 91–95 (2006)
48. Geddes, C.D., Lakowicz, J.R.: Metal-enhanced fluorescence. J. Fluoresc. **12**, 121–129 (2002)
49. Gryczynski, I., Malicka, J., Gryczynski, Z., et al.: Dramatic increases in resonance energy transfer have been observed between fluorophores bound to DNA above metallic silver islands: opportunities for long-range immunoassays and new DNA arrays. J. Fluoresc. **12**, 131–133 (2002)
50. Ray, K., Szmacinski, H., Enderlein, J., et al.: Distance dependence of surface plasmon-coupled emission observed using Langmuir–Blodgett films. Appl. Phys. Lett. **90**, 251116 (2007)
51. Wang, Y.S., Liu, B., Mikhailovsky, A., et al.: Conjugated polyelectrolyte–metal nanoparticle platforms for optically amplified DNA detection. Adv. Mater. **22**, 656–659 (2010)
52. Aslan, K., Huang, J., Wilson, G.M., et al.: Metal-enhanced fluorescence-based RNA sensing. J. Am. Chem. Soc. **128**, 4206–4207 (2006)
53. Zhang, J., Matveeva, E., Gryczynski, I., et al.: Metal-enhanced fluoroimmunoassay on a silver film by vapor deposition. J. Phys. Chem. B **109**, 7969–7975 (2005)
54. Pu, K.Y., Li, K., Liu, B.: Cationic oligofluorene-substituted polyhedral oligomeric silsesquioxane as light-harvesting unimolecular nanoparticle for fluorescence amplification in cellular imaging. Adv. Mater. **22**, 643–646 (2010)
55. Jokerst, J.V., Raamanathan, A., Christodoulides, N., et al.: Nano-bio-chips for high performance multiplexed protein detection: determinations of cancer biomarkers in serum and saliva using quantum dot bioconjugate labels. Biosens. Bioelectron. **24**, 3622–3629 (2009)
56. Ding, C.F., Wang, Z.F., Zhong, H., et al.: Ultrasensitive chemiluminescence quantification of single-nucleotide polymorphisms by using monobase-modified Au and CuS nanoparticles. Biosens. Bioelectron. **25**, 1082–1087 (2010)
57. Li, X.M., Li, W., Zhang, S.S.: Chemiluminescence DNA biosensor based on dual-amplification of thrombin and thiocyanuric acid-gold nanoparticle network. Analyst **135**, 332–336 (2010)
58. Bi, S., Zhou, H., Zhang, S.S.: Bio-bar-code functionalized magnetic nanoparticle label for ultrasensitive flow injection chemiluminescence detection of DNA hybridization. Chem. Commun. **37**, 5567–5569 (2009)

59. Wang, Z.P., Li, J., Liu, B.: CdTe nanocrystals sensitized chemiluminescence and the analytical application. Talanta **77**, 1050–1056 (2009)
60. Jie, G.F., Li, L.L., Chen, C., et al.: Enhanced electrochemiluminescence of CdSe quantum dots composited with CNTs and PDDA for sensitive immunoassay. Biosens. Bioelectron. **24**, 3352–3358 (2009)
61. Hu, X.F., Wang, R.Y., Ding, Y., et al.: Electrochemiluminescence of CdTe quantum dots as labels at nanoporous gold leaf electrodes for ultrasensitive DNA analysis. Talanta **80**, 1737–1743 (2010)
62. Zhou, X.M., Xing, D., Zhu, D.B., et al.: Magnetic bead and nanoparticle based electrochemiluminescence amplification assay for direct and sensitive measuring of telomerase activity. Anal. Chem. **81**, 255–261 (2009)
63. Velev, O.D., Kaler, E.W.: In situ assembly of colloidal particles into miniaturized biosensors. Langmuir **15**, 3693–3698 (1999)
64. Park, S.J., Taton, T.A., Mirkin, C.A.: Array-based electrical detection of DNA with nanoparticle probes. Science **295**, 1503–1506 (2002)
65. Liu, Y., Zhang, D., Evangelyn, C.A., et al.: Biomolecules detection using a silver-enhanced gold nanoparticle-based biochip. Nanoscale Res. Lett. **5**, 533–538 (2010)
66. Wang, J., Xu, D., Kawde, A.N., et al.: Metal nanoparticle-based electrochemical stripping potentiometric detection of DNA hybridization. Anal. Chem. **73**, 5576–5581 (2001)
67. Authier, L., Grossirod, C., Brossier, P., et al.: Gold nanoparticle-based quantitative electrochemical detection of amplified human cytomegalovirus DNA using disposable microband electrodes. Anal. Chem. **73**, 4450–4456 (2001)
68. Cai, H., Xu, Y., Zhu, N., et al.: An electrochemical DNA hybridization detection assay based on a silver nanoparticle label. Analyst **127**, 803–808 (2002)
69. Liao, K., Huang, H.: Femtomolar immunoassay based on coupling gold nanoparticle enlargement with square wave stripping voltammetry. Anal. Chim. Acta **538**, 159–164 (2005)
70. Lee, T.M.H., Li, L.L., Hsing, I.M.: Enhanced electrochemical detection of DNA hybridization based on electrode-surface modification. Langmuir **19**, 4338–4343 (2003)
71. Ozsoz, M., Erdem, A., Kerman, K., et al.: Electrochemical genosensor based on colloidal gold nanoparticles for the detection of factor V Leiden mutation using disposable pencil graphite electrodes. Anal. Chem. **75**, 2181–2187 (2003)
72. Wang, J., Polsky, R., Merkoci, A., et al.: "Electroactive beads" for ultrasensitive DNA detection. Langmuir **19**, 989–991 (2003)
73. Wang, J., Polsky, R., Xu, D.: Silver-enhanced colloidal gold electrochemical stripping detection of DNA hybridization. Langmuir **17**, 5739–5741 (2001)
74. Liao, K.T., Cheng, J.T., Li, C.L., et al.: Ultra-sensitive detection of mutated papillary thyroid carcinoma DNA using square wave stripping voltammetry method and amplified gold nanoparticle biomarkers. Biosens. Bioelectron. **24**, 1899–1904 (2009)
75. Dequaire, M., Degrand, C., Limoges, B.: An electrochemical metalloimmunoassay based on a colloidal gold label. Anal. Chem. **72**, 5521–5528 (2000)
76. Mao, X., Jiang, J., Chen, J., et al.: Cyclic accumulation of nanoparticles: a new strategy for electrochemical immunoassay based on the reversible reaction between dethiobiotin and avidin. Anal. Chim. Acta **557**, 159–163 (2006)
77. Cai, H., Wang, Y., He, P.: Electrochemical detection of DNA hybridization based on silver-enhanced gold nanoparticle label. Anal. Chim. Acta **469**, 165–172 (2002)
78. Chu, X., Fu, X., Chen, K., et al.: An electrochemical stripping metalloimmunoassay based on silver-enhanced gold nanoparticle label. Biosens. Bioelectron. **20**, 1805–1812 (2005)
79. Wang, J., Liu, G., Merkocüi, A.: Electrochemical coding technology for simultaneous detection of multiple DNA targets. J. Am. Chem. Soc. **125**, 3214–3215 (2003)
80. Liu, G., Lee, T.M.H., Wang, J.: Nanocrystal-based bioelectronic coding of single nucleotide polymorphisms. J. Am. Chem. Soc. **127**, 38–39 (2005)
81. Liu, G., Wang, J., Kim, J., et al.: Electrochemical coding for multiplexed immunoassays of proteins. Anal. Chem. **76**, 7126–7130 (2004)

82. Hansen, J.A., Wang, J., Kawde, A., et al.: Quantum-dot/aptamer-based ultrasensitive multi-analyte electrochemical biosensor. J. Am. Chem. Soc. **126**, 2228–2229 (2006)
83. Cheng, W., Yan, F., Ding, L., et al.: Cascade signal amplification strategy for subattomolar protein detection by rolling circle amplification and quantum dots tagging. Anal. Chem. **82**, 3337–3342 (2010)
84. Wang, J.B., Profitt, J.A., Pugia, M.J., et al.: Au nanoparticle conjugation for impedance and capacitance signal amplification in biosensors. Anal. Chem. **78**, 1769–1773 (2006)
85. Tang, H., Chen, J., Nie, L., et al.: A label-free electrochemical immunoassay for carcinoembryonic antigen (CEA) based on gold nanoparticles (AuNPs) and nonconductive polymer film. Biosens. Bioelectron. **22**, 1061–1067 (2007)
86. Bonanni, A., Pividori, M.I., Campoy, S., et al.: Impedimetric detection of double-tagged PCR products using novel amplification procedures based on gold nanoparticles and protein G. Analyst **134**, 602–608 (2009)
87. Zhang, Y., Wang, H., Nie, J.F., et al.: Individually addressable microelectrode arrays fabricated with gold-coated pencil graphite particles for multiplexed and high sensitive impedance immunoassays. Biosens. Bioelectron. **25**, 34–40 (2009)
88. Baca, A.J., Zhou, F.M., Wang, J., et al.: Attachment of ferrocene-capped gold nanoparticle-streptavidin conjugates onto electrode surfaces covered with biotinylated biomolecules for enhanced voltammetric analysis. Electroanalysis **16**, 73–80 (2004)
89. Li, J.H., Hu, J.B., Ding, X.Q., et al.: DNA electrochemical biosensor based on functional gold nanoparticles-amplification. Chem. J. Chin. Univ. **26**, 1432–1436 (2005)
90. Wang, J., Li, J.H., Baca, A.J., et al.: Amplified voltammetric detection of DNA hybridization via oxidation of ferrocene caps on gold nanoparticle/streptavidin conjugates. Anal. Chem. **75**, 3941–3945 (2003)
91. Li, J.H., Hu, J.B.: Functional gold nanoparticle-enhanced electrochemical determination of DNA hybridization and sequence-specific analysis. Acta Chim. Sinica **62**, 2081–2088 (2004)
92. Das, J., Yang, H.J.: Enhancement of electrocatalytic activity of DNA-conjugated gold nanoparticles and its application to DNA detection. J. Phys. Chem. C **113**, 6093–6099 (2009)
93. Li, X.Y., Zhou, Y.L., Zheng, Z.Z., et al.: Glucose biosensor based on nanocomposite films of CdTe quantum dots and glucose oxidase. Langmuir **25**, 6580–6586 (2009)
94. Du, P., Li, H.X., Cao, W.: Construction of DNA sandwich electrochemical biosensor with nano-PbS and nanoAu tags on magnetic microbeads. Biosens. Bioelectron. **24**, 3223–3228 (2009)
95. Liu, X.P., Wu, H.W., Zheng, Y., et al.: A sensitive electrochemical immunosensor for α-Fetoprotein detection with colloidal gold-based dentritical enzyme complex amplification. Electroanalysis **22**, 244–250 (2010)
96. Wu, S., Zhong, Z.Y., Wang, D., et al.: Gold nanoparticle-labeled detection antibodies for use in an enhanced electrochemical immunoassay of hepatitis B surface antigen in human serum. Microchim. Acta **166**, 269–275 (2009)
97. Ambrosi, A., Airo, F., Merkoc, A.: Enhanced gold nanoparticle based ELISA for a breast cancer biomarker. Anal. Chem. **82**, 1151–1156 (2010)
98. Liu, M.Y., Jia, C.P., Huang, Y.Y., et al.: Highly sensitive protein detection using enzyme-labeled gold nanoparticle probes. Analyst **135**, 327–331 (2010)
99. Ding, C.F., Li, H., Hu, K.C., et al.: Electrochemical immunoassay of hepatitis B surface antigen by the amplification of gold nanoparticles based on the nanoporous gold electrode. Talanta **80**, 1385–1391 (2010)
100. Bi, S., Yan, Y.M., Yang, X.Y., et al.: Gold nanolabels for new enhanced chemiluminescence immunoassay of alpha-fetoprotein based on magnetic beads. Chem. Eur. J. **15**, 4704–4709 (2009)
101. Fang, L.Y., Lü, Z.Z., Wei, H., et al.: A electrochemiluminescence aptasensor for detection of thrombin incorporating the capture aptamer labeled with gold nanoparticles immobilized onto the thio-silanized ITO electrode. Anal. Chim. Acta **628**, 80–86 (2008)
102. Zhu, Z.Q., Su, Y.Y., Li, J., et al.: Highly sensitive electrochemical sensor for mercury(II) ions by using a mercury-specific oligonucleotide probe and gold nanoparticle-based amplification. Anal. Chem. **81**, 7660–7666 (2009)

103. Ono, A., Togashi, H.: Highly selective oligonucleotide-based sensor for mercury(II) in aqueous solutions. Angew. Chem. Int. Ed. **43**, 4300–4302 (2004)
104. Ding, C.F., Zhang, Q., Lin, J.M., et al.: Electrochemical detection of DNA hybridization based on bio-bar code method. Biosens. Bioelectron. **24**, 3140–3143 (2009)
105. Ding, C.F., Ge, Y., Lin, J.M.: Aptamer based electrochemical assay for the determination of thrombin by using the amplification of the nanoparticles. Biosens. Bioelectron. **25**, 1290–1294 (2010)
106. Shen, L., Chen, Z., Li, Y., et al.: Electrochemical DNAzyme sensor for lead based on amplification of DNA-Au bio-bar codes. Anal. Chem. **80**, 6323–6328 (2008)
107. Mani, V., Chikkaveeraiah, B.V., Patel, V., et al.: Ultrasensitive immunosensor for cancer biomarker proteins using gold nanoparticle film electrodes and multienzyme-particle amplification. ACS Nano **3**, 585–594 (2009)
108. Carrillo-Carrión, C., Simonet, B.M., Valcárcel, M.: Carbon nanotube–quantum dot nanocomposites as new fluorescence nanoparticles for the determination of trace levels of PAHs in water. Anal. Chim. Acta **652**, 278–284 (2009)
109. Lai, G.S., Yan, F., Ju, H.X.: Dual signal amplification of glucose oxidase-functionalized nanocomposites as a trace label for ultrasensitive simultaneous multiplexed electrochemical detection of tumor markers. Anal. Chem. **81**, 9730–9736 (2009)
110. Lee, A.C., Ye, J.S., Tan, S.N., et al.: Carbon nanotube-based labels for highly sensitive colorimetric and aggregation-based visual detection of nucleic acids. Nanotechnology **18**, 455102 (2007)
111. Wang, Y.Y., Liu, B.: Conjugated polymer as a signal amplifier for novel silica nanoparticle -based fluoroimmunoassay. Biosens. Bioelectron. **24**, 3293–3298 (2009)
112. Yang, M.H., Li, H., Javadi, A., et al.: Multifunctional mesoporous silica nanoparticles as labels for the preparation of ultrasensitive electrochemical immunosensors. Biomaterials **31**, 3281–3286 (2010)
113. Zanarini, S., Rampazzo, E., Ciana, L.D.: $Ru(bpy)_3^{2+}$ covalently doped silica nanoparticles as multicenter tunable structures for electrochemiluminescence amplification. J. Am. Chem. Soc. **131**, 2260–2267 (2009)
114. Chen, L.Y., Chen, C.L., Li, R.N., et al.: CdTe quantum dot functionalized silica nanosphere labels for ultrasensitive detection of biomarker. Chem. Commun. **19**, 2670–2672 (2009)
115. Dong, H.F., Yan, F., Ji, H.X., et al.: Quantum-dot-functionalized poly(styrene-co-acrylic acid) microbeads: step-wise self-assembly, characterization, and applications for sub-femtomolar electrochemical detection of DNA hybridization. Adv. Funct. Mater. **20**, 1173–1179 (2010)
116. Tang, D.P., Su, B.L., Tang, J., et al.: Nanoparticle-based sandwich electrochemical immunoassay for carbohydrate Antigen 125 with signal enhancement using enzyme-coated nanometer-sized enzyme-doped silica beads. Anal. Chem. **82**, 1527–1534 (2010)

http://www.springer.com/978-1-4419-9621-3

NanoBiosensing
Principles, Development and Application
Ju, H.; Xueji, Z.; Wang, J.
2011, XV, 586 p., Hardcover
ISBN: 978-1-4419-9621-3